ISET Journal of Earthquake Technology, Paper No. 575, Vol. 59, No. 4, Dec. 2022, pp. 151-178

SKEW PLATE VIBRATION ANALYSIS USING MODIFIED VLASOV MODEL AND HIGHER-ORDER FINITE ELEMENT

Ashis Kumar Dutta (Corresponding Author)
PhD Scholar, Department of Construction Engineering, Jadavpur University, Salt Lake, Kolkata, 700098, India
Email id: *dutta.ashis2013@gmail.com, ORCID identifier 0000-0001-6424-2584*

Debasish Bandyopadhyay
Professor, Department of Construction Engineering, Jadavpur University, Salt Lake, Kolkata, 700098, India
Email id:*dban65@yahoo.com*

Jagat Jyoti Mandal
Ex-Professor, Department of Civil Engineering, National Institute of Technical Teachers' Training and Research, Kolkata, 700106, India, Email id:*jjm_civil03@yahoo.co.in*

ABSTRACT

Skew-plate is unavoidable in aerospace, civil, and mechanical engineering. It is challenging to ascertain how significant the dynamic response on a skew plate on an elastic foundation is. This study uses a higher-order finite element method and the modified Vlasov model to investigate the vibration of a four-nodded skewed plate on an elastic foundation. A Matlab algorithm has been written to tackle the boundary conditions within the present formulation. The code undergoes validation through convergence studies. The findings demonstrate a significant level of concordance with previous research. Additionally, a parametric analysis provided tabular and graphical representations of the first ten natural frequency characteristics. Based on the study, the present method is straightforward and excellent for skew plates on Vlasov foundations. It has a reasonable convergence rate, is precise, and requires little computation time and effort. Numerical results of free vibration analysis of skewed plates resting on elastic foundations for various support conditions will demonstrate the effectiveness of the present elements to provide multiple results and serve as a handy reference for future practitioners and design engineers in this field.

KEYWORDS: Skewed Plate; Modified Vlasov Model; Higher-order Finite Element; Frequency Parameter

INTRODUCTION

Free vibration analysis of skewed plates resting on elastic foundations has limited applications. Still, it is unavoidable in aerospace, civil, and mechanical engineering. Unfortunately, there are few research papers on vibration analysis of skewed plates on the Vlasov foundation. It is challenging to ascertain how dynamic vertical or horizontal forces are transferred to the foundation due to these designs' significant difficulties with soil-structure interaction. As a result, structures of various forms, such as beams, plates, and shells made of multiple materials, are widely used. Steel-bearing vessels on concrete, bridges, ships, and other technical challenges may all be reduced to beams, plates, and shells on elastic foundations. This requires a careful investigation of skew plates on Vlasov foundations. Although most finite element software can tackle this issue, analytical approaches provide several advantages for understanding the core ideas of physics and mechanics. Numerous theoretical frameworks for structures with elastic foundations have been developed due to significant research into the interaction between frames and complex media. Analytical approaches often relate to problems that can be solved on paper using closed-form equations. Analytical procedures are often regarded as yielding the most insightful results due to their ability to explain the relationship between variables accurately using mathematical equations. The "proof" of an analytical solution to a problem is a set of defensible logical procedures that may be used to confirm that the answer is correct. Numerical approaches are used since most of the above mentioned issues cannot be solved analytically.

Numerous studies have been conducted to predict how elastic foundations affect the plate. The assumption that each foundation point's reaction forces per unit area correspond to the foundation's deflection forms the basis of Winkler's relatively simple model [1]. Unfortunately, the Winkler model has a problem that accounts for most of the difference between the soil outside the structure and the soil underneath the system, and soil displacement occurs by including a second spring that interacts with the

Winkler model's initial spring to support the soil medium's displacement continuity, Hetenyi [1], Filonenko-Borodich [2], and Pasternak [3] developed two-parameter foundation models to address the shortcomings of the Winkler model. A multitude of parameters influence sub-grade response, making the mechanical modelling of skewed plate-subsoil interaction problems a complex mathematical phenomenon. The analytical solution techniques for skew plates have been comprehensively reviewed by Morley [4]. Butalia et al. [5] used the nine-noded Heterosis element to study skew plates for different skew angles, stress conditions, and support requirements. Sengupta [6] examined the skew plate's performance using a particular three-noded element. Two more elements, element A and element B, created by Sengupta [7, 8], are used to compare the outcomes. In detail, Srinivasa et al. [9] investigate the bending behaviour of supported skew plates. Liew and Han [10] present the differential quadrature-based bending analysis of a thick, simply supported skew plate. Few researchers have addressed skewed plates on an elastic foundation as there is mathematical complexity. Chun and Lim [11] investigated the behaviour of isotropic and orthotropic thick skewed plates on elastic foundations. Chun and Ohga [12] examined the analytical method to predict the bending behaviour of skewed thick plates on the Winkler foundation in detail. Xenalevina Sidara and Maknun [13] study the convergence behaviour of DKMQ elements in functionally graded material skew plates. Hassan and Kurgan [14] used the extended Kantorovich approach to investigate the buckling analysis of thin skew isotropic plates resting on a Pasternak foundation. Wang and Yuan [15] studied the buckling analysis of thin skew isotropic plates under general in-plane loads by the modified differential quadrature method. Joodaky and Joodaky [16] developed semi-analytical solutions to the behaviour of skew plates on Pasternak and Winkler foundations. A thorough examination of homogeneous and FGM skew plates resting on varied Winkler-Pasternak elastic foundations has been conducted using free vibration analysis by Ketabdari et al.[17]. Vallabhan and Das [18] used an iterative process to determine a third parameter, γ, as a function of the foundational and structural characteristics. The parameters of this model, which they termed the modified Vlasov model, as well as the loading type, intensity, and depth, all depend on the soil characteristics and structure. Özgan K, Daloğlu [19] address the free vibration analysis of thick plates resting on elastic foundations using the modified Vlasov model with higher-order finite elements. Hamarat et al. [20] analyze the seismic behaviour of a 3-D frame superstructure and a mat foundation resting on an elastic foundation using the modified Vlasov model via the finite element technique. Buczkowski et al. [21] employed the mixed first-order transverse 16-node locking-free Mindlin plate resting on a two-parameter elastic foundation to solve the eigenvalue issue and determine the natural frequencies of the plate. Finally, Gibigaye et al. [22] used the discrete singular convolution method to analyze the free vibration of a rectangular, isotropic thin plate with dowels on a modified Vlasov foundation. Dutta et al. [23] developed a higher-order finite element method for vibration analysis of beams on elastic foundations. Bogner et al. [24] considered one additional degree of freedom (DOF) per node leads to four nodded sixteen DOF elements.

Extensive vibration analysis of four-noded skew plates resting on elastic foundations for different support conditions using the modified Vlasov model is presented using higher-order finite elements. Excellent conformity is demonstrated by a validation and convergence study of the suggested formulation conducted using a Matlab [25] code. Performance, convergence rate, accuracy, and application of the present element are all excellent and without issue.

LIST OF SYMBOLS/NOTATIONS

L/a = Length of plate.
B/b = Width of plate.
E_s, v_s, ρ_s = Young's modulus of elasticity, Poisson's ratio and mass density of soil.
q = load per unit area in the vertical-direction.
H = thickness of the subsoil.
G_b = Foundation shear parameter.
K= Foundation Winkler parameter.
γ = Decay parameter.
N = Shape function.
m_1= Mass per unit area of the plate.
c = Damping constant.
ω = Circular Frequency.

τ = Frequency parameter.
ϕ = Dimensionless vertical soil displacement function.
E_o, ν_o = Effective modulus of elasticity and Poisson's ratio of soil.
m_0 = The equivalent mass of soil participating in vibration.
w = The plate's displacement.
$\ddot{w}$ = Acceleration.
[M] = The mass matrices of the plate-soil system.
[KK] = The stiffness matrices of the plate-soil system.
ρ = Mass density of plate material.
D = Plate's flexural rigidity.
h = The plate's thickness.
E = Young's modulus of plate material.
v = Poisson's ratio of plate material
PS = Present study.
β = The skew angle of plate.

METHODOLOGY

1 Modified Vlasov Model

Filonenko Borodich (1940) tried connecting the springs' top ends to a stretched elastic membrane with a constant tension T. The relation between load, q, and deflection, w, in this model, is defined as $q = Kw - T\nabla^2 w$ Although this is appropriate, no method was provided for calculating K and T, except by extensive experiment and empirical correlation. Realizing that the soil continuum is subjected to shear strains in addition to vertical strains, Pasternak (1954) developed a model in which he assumed a shear interaction between springs by connecting the ends of the springs to a beam or plate consisting of incompressible vertical elements which deform only by lateral shear. The load-deflection relation in Pasternak's is given by $q = Kw - G\nabla^2 w$ where G represents the shear modulus of the elastic foundation. Vlasov and Leont'ev (1966) tried to use a new mathematical approach to solve the above problem. Using a variational method, they developed a two-parameter model for plates on elastic foundations. This method accounted for the neglected shear strain within the soil continuum. The relation between displacement, w, and load, q, is given in this model by $D\nabla^4 w + Kw - G_b\nabla^2 w = q$, where G_b is the soil-shear parameter and all the other terms are as previously defined. To calculate these parameters, Vlasov and Leont'ev introduced another parameter, γ, to characterize the vertical deformation profile within the soil continuum. The advantage of Vlasov and Leont'ev's approach is the elimination of the necessity to determine the values of the subgrade reaction, K, and shear parameter, G_b, arbitrarily because these values can be computed from the material properties, modulus of elasticity, Poisson's ratio and mass density (E_s, ν_s, ρ_s) and the thickness of the subsoil (H). By choosing an arbitrary value for γ, Vlasov and Leont'ev assumed a displacement pattern of the soil medium; however, the authors did not offer a method for determining γ. An iterative approach for determining the γ parameter for beams on an elastic foundation was devised by Vallabhan and Das [18]. They defined every parameter that affects K and G_b values. They showed that the value of γ also depends on the ratio of the soil depth to the beam length for evenly distributed loads. Their model became known as the modified Vlasov model. The distribution of the loading on the plate, the geometry of the structure, the depth of the stratum, and the material properties of the soil and the structure all influenced these characteristics.

By adding a third parameter, γ, to describe the vertical deformation profile within the soil continuum, Selvaduari [26], Vlasov, and Leont'ev [27] created a novel concept of the two-parameter model that has the advantage of determining soil parameters and dynamically activated mass depending on soil material properties, modulus of elasticity, Poisson's ratio and mass density (E_s, ν_s, ρ_s) and the thickness of the subsoil (H). By utilizing an iterative process, Vallabhan and Das [18] identified the parameter as a function of the foundational and structural characteristics and gave this model the name "modified Vlasov model." The parameters rely on the structure, the rigid base's depth, the soil's features, and the kind and amount of loads (Figure 1).

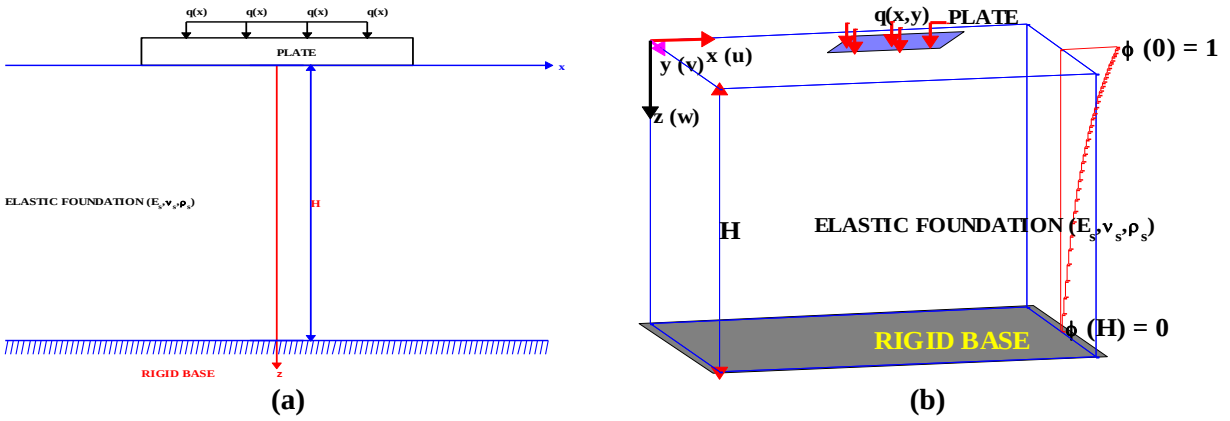

Fig. 1(a, b) Finite plates rest on a two-parameter Vlasov foundation

2 Dynamic Equation of Plates on Vlasov Foundation

$D\nabla^4 w + Kw - G_b\nabla^2 w = q$ is the static equation of the plate on a two-parameter elastic foundation. After applying D'Alembert's principle, the unbalanced force equals the inertia force.

$$\text{Unblanced force} = q(x,y,t) - (D\nabla^4 w - G_b\nabla^2 w + Kw) \quad (1)$$

$$\text{And inertia force } m\frac{\partial^2 w}{\partial t^2} \quad (2)$$

$$\therefore m\frac{\partial^2 w}{\partial t^2} = q(x,y,t) - (D\nabla^4 w - G_b\nabla^2 w + Kw) \quad (3)$$

Considering the damping force $\left(c\frac{\partial w}{\partial t}\right)$ Also, it gets the following.

$$(D\nabla^4 w - G_b\nabla^2 w + Kw) + c\frac{\partial w}{\partial t} + (m_1 + m_0)\frac{\partial^2 w}{\partial t^2} = q(x,y,t) \quad (4)$$

It is the plate's dynamic equation on the Vlasov foundation.

m_1 - Mass per unit plate area = ρh, ρ - mass density of plate material, and c - Damping constant.

Where D is the plate's flexural rigidity, m_1 is the plate's mass per unit area = ρh, ρ - mass density of the plate material, h is the plate's thickness, c is the damping constant, and q is the lateral force per unit area acting on the plate. The soil parameters K, G_b, and m_0 are listed in [19, 22, 27], and $\phi(z)$ is a dimensionless function that illustrates how the vertical soil displacement decreases with depth.

The variation of φ as $\varphi(z) = \frac{\sinh\gamma(1-\frac{z}{H})}{\sinh\gamma}$

$$K = \int_0^H \frac{E_0}{(1-{v_0}^2)}\left(\frac{d\varphi}{dz}\right)^2 dz,\ G_b = \int_0^H \frac{E_0}{2(1+v_0)}\varphi^2(z)\,dz,\ m_0 = \int_0^H \rho_s\varphi^2(z)\,dz,\ E_0 = \frac{E_s}{(1-{v_s}^2)} \text{ and } v_0 = \frac{v_s}{(1-v_s)} \quad (5)$$

E_s, ν_s = Young's modulus of elasticity and Poisson's ratio of soil.

E_0, ν_0 = Effective modulus of elasticity and Poisson's ratio of soil.

Where ρ_s is the mass density of the soil.

$$K = \frac{E_s(1-v_s)\gamma}{(1+v_s)(1-2v_s)H}\left(\frac{\sinh\gamma\cosh\gamma+\gamma}{2\sinh^2\gamma}\right) \quad (6)$$

$$G_b = \frac{E_s H}{2\gamma(1+v_s)}\left(\frac{\sinh\gamma\cosh\gamma-\gamma}{2\sinh^2\gamma}\right) \quad (7)$$

$$m_0 = \frac{\rho_s H}{\gamma}\left(\frac{\sinh\gamma\cosh\gamma-\gamma}{2\sinh^2\gamma}\right) \quad (8)$$

For thin layer variation, φ may be assumed as $\varphi(z) = \left(1-\frac{z}{H}\right)$

$$K = \frac{E_s(1-v_s)}{H(1+v_s)(1-2v_s)},\ G_b = \frac{E_s H}{6(1+v_s)},\ m_0 = \frac{\rho_s H}{3} \quad (9)$$

γ parameter denotes the vertical deformation within the subsoil. Where m_0 - is the equivalent mass of soil participating in vibration.

The critical point here is that the modulus of sub-grade reaction, K, the second parameter, G_b, which represents the shear deformation of the soil, and m_0 all depend on the vertical deformation function, γ, and the depth of the soil, H. More details of the modified Vlasov model are available in [28–32].

Equivalent boundary forces exist at the nodes due to the infinite soil domain on the plate boundary Turhan [28].

For the corner node, $R = 0.75 \times G_b \times w$ and other nodes, $Q = a\sqrt{G_b K}\,w$ where w is the relevant

boundary node's deflection. Stiffness for corner node $= \frac{3}{4} G_b$ and for other nodes stiffness $= a\sqrt{G_b K}$. Where 'a' is the node's tributary Length. The effect at the corner node of the soil region is modelled by adding $3G_b/4$ to the stiffness term, and for the remaining nodes $a\sqrt{G_b K}$.

3 Characteristic Equation

Applying the Hamiltonian According to Petyt [33], the plate-soil equations of motion for free vibration in the absence of damping are

$$[M]\{\ddot{w}\} + [KK]\{w\} = \{0\} \quad (10)$$

Where [KK] and [M] are the stiffness and mass matrices of the plate-soil system, and w is the plate's displacement and ẅacceleration, respectively. By solving the generalized Eigenvalue problems, one can obtain the natural frequencies and vibrational mode, as stated by Hinton [34].
For free vibration analysis, if a harmonic motion is assumed, then

$$\{w\} = \{\bar{w}\}e^{i\omega t} \text{ and } \{\ddot{w}\} = -\omega^2\{\bar{w}\}e^{i\omega t} \quad (11)$$

Where $\{\bar{w}\}$ is the amplitude of $\{w\}$.

When $\{w\}$ and $\{\ddot{w}\}$ are substituted in equation (10), one obtains

$$([KK] - \omega^2[M])\{\bar{w}\} = \{0\} \quad (12)$$

The non-trivial approach of equation (12) suggests that the deciding equation is $|([KK] - \omega^2[M])| = 0$. 'ω' stands for the frequency of nature.

4 Finite Element Formulation

Each of the four corner nodes is represented by four DOFs, as seen in Figure 2. This means that the element has sixteen DOFs in total. Shape functions are obtained by accurately multiplying first-order cubic Hermitian functions in the x and y axes of a skewed 16 DOF plate element. For details, Dutta et al. [35].

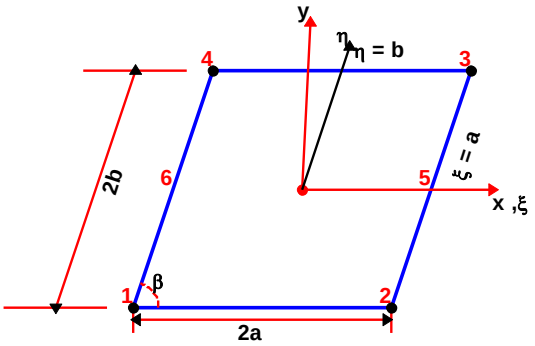

Fig. 2 PBS4 in oblique coordinate

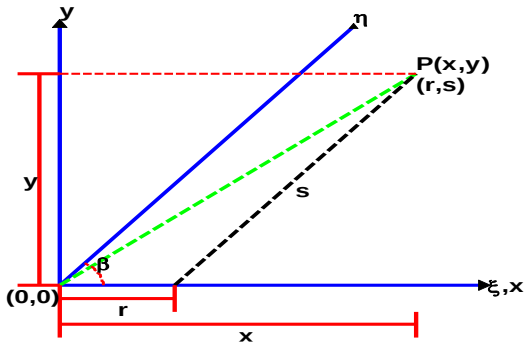

Fig.3 Point in global and local coordinate system

As seen in Figure 3, x = r + scos β, y = ssin β, or s = ycosec β, and r = x - ycot β, with β being the skew angle with respect to the horizontal $u(x,y,z) = -z\frac{\partial w_0}{\partial x}$; $v(x,y,z) = -z\frac{\partial w_0}{\partial y}$ and $w(x,y,z) = w_0(x,y)$. Furthermore, it is assumed that w (x, y, 0) = w (x,y). The variations in displacements of the soil's surface and the plate's centre surface are equal.

At the ith node the nodal displacement is $\{\delta_i\} = \left\{w_i \quad \left(\frac{\partial w}{\partial x}\right)_i \quad \left(\frac{\partial w}{\partial y}\right)_i \quad \left(\frac{\partial^2 w}{\partial x \partial y}\right)_i\right\}^T$.For four nodded elements, the element displacement vector is defined as $\{d_e\} = \{d_1 d_2 d_3 d_4\}^T$. The thin plate concept forms the framework of the element. Therefore, requiring a variation in transverse displacement w on the element region is adequate. $(1+x+x^2+x^3)(1+y+y^2+y^3)$ is the full product of a cubic polynomial in both the x and y directions. A 16 d.o.f. It skewed the plate component. First-order cubic Hermitian functions are properly multiplied in both the x and y axes to provide shape functions.

The strain displacement relation for plane stress condition is given by

$$\frac{\partial r}{\partial x} = 1, \frac{\partial r}{\partial y} = -\cot\beta, \frac{\partial s}{\partial x} = 0, \frac{\partial s}{\partial y} = \text{cosec}\,\beta \quad (13)$$

$$\frac{\partial w_0}{\partial x}=\frac{\partial w_0}{\partial r}\frac{\partial r}{\partial x}+\frac{\partial w_0}{\partial s}\frac{\partial s}{\partial x}=\frac{\partial w_0}{\partial r}\times 1+\frac{\partial w_0}{\partial s}\times 0=\frac{\partial w_0}{\partial r}\therefore\frac{\partial}{\partial x}=\frac{\partial}{\partial r}\text{ and }\frac{\partial^2 w_0}{\partial x^2}=\frac{\partial^2 w_0}{\partial r^2} \quad (14)$$

$$\frac{\partial w_0}{\partial y}=\frac{\partial w_0}{\partial r}\frac{\partial r}{\partial y}+\frac{\partial w_0}{\partial s}\frac{\partial s}{\partial y}=\frac{\partial w_0}{\partial r}\times(-\cot\beta)+\frac{\partial w_0}{\partial s}\times\operatorname{cosec}\beta=-\cot\beta\frac{\partial w_0}{\partial r}+\operatorname{cosec}\beta\frac{\partial w_0}{\partial s} \quad (15)$$

$$\therefore\frac{\partial}{\partial y}=-\cot\beta\frac{\partial}{\partial r}+\operatorname{cosec}\beta\frac{\partial}{\partial s}\text{ and }\frac{\partial^2 w_0}{\partial y^2}=\frac{\partial}{\partial y}\left(-\cot\beta\frac{\partial w_0}{\partial r}+\operatorname{cosec}\beta\frac{\partial w_0}{\partial s}\right) \quad (16)$$

$$\therefore\frac{\partial^2 w_0}{\partial y^2}=\cot^2\beta\frac{\partial^2 w_0}{\partial r^2}-2\operatorname{cosec}\beta\cot\beta\frac{\partial^2 w_0}{\partial r\,\partial s}+\operatorname{cosec}^2\beta\frac{\partial^2 w_0}{\partial s^2}\text{ and }\frac{\partial^2 w_0}{\partial x\,\partial y}=-\cot\beta\frac{\partial^2 w_0}{\partial r^2}+\operatorname{cosec}\beta\frac{\partial^2 w_0}{\partial r\,\partial s} \quad (17)$$

Hence, generalized curvatures are written.

$$\begin{Bmatrix}\chi_x\\ \chi_y\\ \chi_{xy}\end{Bmatrix}=\begin{bmatrix}\frac{\partial^2 w_0}{\partial x^2}\\ \frac{\partial^2 w_0}{\partial y^2}\\ 2\frac{\partial^2 w_0}{\partial x dy}\end{bmatrix}=\begin{bmatrix}1 & 0 & 0\\ \cot^2\beta & \operatorname{cosec}^2\beta & -2\operatorname{cosec}\beta\cot\beta\\ -2\cot\beta & 0 & 2\operatorname{cosec}\beta\end{bmatrix}\begin{bmatrix}\frac{\partial^2 w_0}{\partial r^2}\\ \frac{\partial^2 w_0}{\partial s^2}\\ \frac{\partial^2 w_0}{\partial r\,\partial s}\end{bmatrix} \quad (18)$$

$$\begin{Bmatrix}\chi_x\\ \chi_y\\ \chi_{xy}\end{Bmatrix}=\begin{bmatrix}\frac{\partial^2 N}{\partial r^2} & 0 & 0\\ \cot^2\beta\frac{\partial^2 N}{\partial r^2} & \operatorname{cosec}^2\beta\frac{\partial^2 N}{\partial s^2} & -2\operatorname{cosec}\beta\cot\beta\frac{\partial^2 N}{\partial r\,\partial s}\\ -2\cot\beta\frac{\partial^2 N}{\partial r^2} & 0 & 2\operatorname{cosec}\beta\frac{\partial^2 N}{\partial r\,\partial s}\end{bmatrix}\{w\} \quad (19)$$

$$\therefore[B_{bi}]=\begin{bmatrix}\frac{\partial^2 N}{\partial r^2} & 0 & 0\\ \cot^2\beta\frac{\partial^2 N}{\partial r^2} & \operatorname{cosec}^2\beta\frac{\partial^2 N}{\partial s^2} & -2\operatorname{cosec}\beta\cot\beta\frac{\partial^2 N}{\partial r\,\partial s}\\ -2\cot\beta\frac{\partial^2 N}{\partial r^2} & 0 & 2\operatorname{cosec}\beta\frac{\partial^2 N}{\partial r\,\partial s}\end{bmatrix} \quad (20)$$

$[B_b]=[B_{b1}B_{b2}\dots\dots\dots B_{b16}]$ For four nodded elements.

Stresses are related to strain in terms of elasticity matrix for plane stress condition given by

$$C_{11}=\frac{E}{(1-\nu^2)}\text{ and }G=\frac{E}{2(1+\nu)}; \quad (21)$$

$$C_{22}=C_{11};C_{33}=C_{11};C_{12}=\nu C_{11};C_{13}=C_{12};C_{21}=C_{12};C_{23}=C_{12};C_{31}=C_{12};C_{32}=C_{12};C_{44}=G; \quad (22)$$

$$\therefore[C_b]=\begin{bmatrix}C_{11} & C_{12} & 0\\ C_{21} & C_{22} & 0\\ 0 & 0 & C_{44}\end{bmatrix};[D]=\int_{-\frac{h}{2}}^{\frac{h}{2}}z^2[C_b]\,dz\text{ where [D] is the Plate rigidity matrix.}$$

$$[D]=\frac{Eh^3}{12(1-\nu^2)}\begin{bmatrix}1 & \nu & 0\\ \nu & 1 & 0\\ 0 & 0 & \frac{1-\nu}{2}\end{bmatrix} \quad (23)$$

Hence, the bending stiffness matrix,

$$[K_b]=[B]^T[D][B]=\int_{-1}^{1}\int_{-1}^{1}[B_b]^T[D][B_b]|J|dsdt \quad (24)$$

and |J| = absinβ. Following the usual steps, the bending is expressed as

$$[K_b]=\sum_{j=1}^{4}\sum_{i=1}^{4}W_iW_j|J|[B_b]^T[D][B_b] \quad (25)$$

The entire 4 × 4 Point Gauss-Legendre type quadrature is utilised for bending stiffness, as these equations demonstrate.

The lateral deflection of area 'dA' normal to the foundation is given by a structural element with a differential area 'dA' in contact with the foundation is w = [N]{d }

The strain energy U_r in a linear spring is given by eq. $=\frac{1}{2}Kw^2$

$U_r=\frac{1}{2}\int Kw^2\,dA$; K is the soil parameter known as the modulus of the sub-grade reaction.

$$\text{Strain energy, }U_r=\frac{1}{2}\int K\{d\}^T[N]^T[N]\{d\}\,dA=\frac{1}{2}\{d\}^T[K_f]\{d\}k \quad (26)$$

In which the foundation stiffness matrix for the element is, $[K_f]=\int K[N]^T[N]\,dA$

$$[K_f]=Kabsin\beta\int_{-1}^{1}\int_{-1}^{1}[N]^T[N]\,dsdt=K\int_{-1}^{1}\int_{-1}^{1}[N]^T[N]\,|J|dsdt \quad (27)$$

A typical sub-matrix for the foundation parameter corresponding to the i^{th} node is

$[K_{fi}]=K\sum_{i=1}^{4}\sum_{j=1}^{4}W_iW_j|J|N_i{}^TN_j=\{K_{f1}K_{f2}\dots\dots\dots\dots K_{f16}\}^T$ For four nodded four DOF/node elements.

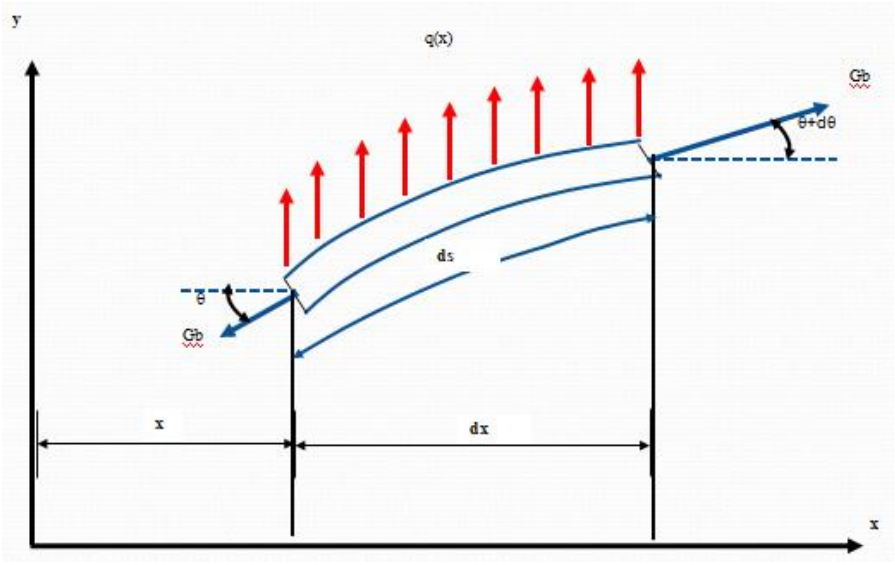

Fig. 4 Length of differential element 'dx' in deformed position, 'ds'

$ds = \sqrt{(dx)^2 + (dw)^2} = dx\sqrt{1 + \left(\frac{dw}{dx}\right)^2}\ dx\left[1 + \left(\frac{dw}{dx}\right)^2\right]^{\frac{1}{2}} = dx\left[1 + \frac{1}{2}\left(\frac{dw}{dx}\right)^2\right] \therefore ds - dx = \frac{1}{2}\left(\frac{dw}{dx}\right)^2$ (Figure 4). Strain energy stored by foundation parameter 'G_b' is given by Rao [36]

$$U = \frac{1}{2}\int_{-a}^{a} Gb\left(\frac{\partial w}{\partial x}\right)^2 dx = \frac{1}{2}\int_{-a}^{a} G_b\{d\}^T[N']^T[N']\{d\}\,dx = \frac{1}{2}\{d\}^T[K_{ex}]\{d\} \text{ where } [K_{ex}] = \int_{-a}^{a} G_b[N']^T[N']dx \text{ Similarly, for y-direction, } \left[K_{ey}\right] = \int_{-b}^{b} G_b[N']^T[N']dy$$

$R = [N'] = \frac{\partial N}{\partial x}$ and $S = [N'] = \frac{\partial N}{\partial y}$. So, the stiffness for the shear parameter, G_b, is $[K_e] = G_b \iint [S^T S + R^T R]dA$

$$[K_e] = G_b \int_{-1}^{1}\int_{-1}^{1}\left(\frac{1}{a^2}\left[\frac{\partial N}{\partial s}\right]^T\left[\frac{\partial N}{\partial s}\right] + \frac{1}{b^2}\left[\frac{\partial N}{\partial t}\right]^T\left[\frac{\partial N}{\partial t}\right]\right)|J|dsdt = G_b ab \sin\beta \int_{-1}^{1}\int_{-1}^{1}\left(\frac{1}{a^2}\left[\frac{\partial N}{\partial s}\right]^T\left[\frac{\partial N}{\partial s}\right] + \frac{1}{b^2}\left[\frac{\partial N}{\partial t}\right]^T\left[\frac{\partial N}{\partial t}\right]\right)dsdt \quad (28)$$

Additionally, a typical sub-matrix for the i[th] nodes for the second foundation parameter is

$$\left[K_{e_i}\right] = G_b\left(\sum_{i=1}^{4}\sum_{j=1}^{4} W_i W_j |J| \frac{dN}{dx_i} + \sum_{i=1}^{4}\sum_{j=1}^{4} W_i W_j |J| \frac{dN}{dy_i}\right) \quad (29)$$

When it comes to elements with four nodes, $[K_e] = [K_{e1} K_{e2} \ldots\ldots K_{e16}]$.
Elements The stiffness matrix is

$$[KK] = [K_b] + [K_f] + [K_e] \quad (30)$$

The global stiffness matrix is generated by using the conventional finite element method.

$$\therefore [K_S] = \sum_1^n([K_b] + [K_f] + [K_e]) \quad (31)$$

5 Mass Matrix

Additionally, vibration does not cause the subsoil to vary in depth.
The thin plate's kinetic energy is defined by

$$T_e = \frac{1}{2}\rho \int_{A_e}\left(\int_{\frac{-h}{2}}^{\frac{h}{2}} \dot{w}^2 dz\right)dA = \frac{1}{2}\rho h \int_{A_e} \dot{w}^2\, dA = \frac{1}{2}\{d'\}^T(\rho h + m_0)\int_0^l [N]^T\,[N]dA\{d'\} \quad (32)$$

$$\therefore [M] = (\rho h + m_0)\int_{A_e}[N]^T[N]dA \quad (33)$$

$$\therefore [M] = (\rho h + m_0)ab\sin\beta \int_{-1}^{1}\int_{-1}^{1}[N]^T[N]\,dsdt = (\rho h + m_0)\int_{-1}^{1}\int_{-1}^{1}[N]^T[N]\,|J|\,dsdt \quad (34)$$

CONVERGENCE STUDY

This study considers several boundary conditions, such as SSSS, CCCC, and FFFF, where S refers to

a simply-supported edge, F to a free edge, and C to a clamped edge. Clamped edge, $w = \frac{\partial w}{\partial x} = \frac{\partial w}{\partial y} = \frac{\partial^2 w}{\partial x \partial y} = 0$, simply supported edge, w = 0 and free edge, $w \neq 0, \frac{\partial w}{\partial x} \neq 0, \frac{\partial w}{\partial y} \neq 0, \frac{\partial^2 w}{\partial x \partial y} \neq 0$.

For example, CFSC means that edge (Figure 2): (ξ = - a) is clamped, edge: (η = - b) is free, edge: (ξ = a) is simply supported, and edge (η = - b) is clamped.

The skew angle β is defined as the angle that the oblique edge of the plate makes with the horizontal, as shown in Figure 2.

A skewed plate (a/b = 1) is divided into 20 intervals in Length and breadthwise, i.e., 400 elements and 441 nodes in the mesh. A mesh size of 20 × 20 ($\frac{a}{20}$ *and* $\frac{b}{20}$) is applied throughout the article following the Convergence analysis for a fair result.

A skewed plate (a/b = 1) on an elastic foundation (Kw = 100, Ks = 100 where $Kw = Ka^2b^2/D$ and $Ks = G_b ab/D$) is initially investigated to validate the current formulation. A convergence analysis is carried out simultaneously for the clamped, simply supported, and free plate. For free vibration analysis, a mesh size of 20 × 20 rather than 30 × 30 ($\frac{a}{30}$ *and* $\frac{b}{30}$) of a three DOF per node skewed plate element is chosen for a good result, using less computer memory, time, and resources. The frequency parameter, $\tau_s = \omega_s a^2 \sqrt{\frac{\rho h}{D}}$ Where s is the mode number compared with the results from Ketabdari et al.[17] and tabulated in Table 1 and presented in Figures 5-7. This table and figures show the proposed formulation's rapid convergence, observed for simply supported plate, and free plate converges from the reverse direction. One translation mode and two rotation modes result from a normal modes analysis without loads or constraints. The modal frequencies of the first three modes are zero or almost zero. Thus, there is no vibration in this rigid body motion. That is why the fourth mode for a free plate was considered.

Table 1: Convergence study for natural frequency of CCCC, SSSS plate for 1st mode, and FFFF plate for 4th mode

Mesh Size	CCCC	SSSS	FFFF
	τ_1	τ_1	τ_4
4 × 4	70.5631	52.2650	62.7920
8 × 8	69.2022	52.4650	64.3773
12 × 12	68.9118	52.4899	64.7932
16 × 16	68.8018	52.4986	64.9720
18 × 18	68.7707	52.5011	65.0270
20 × 20	68.7478	52.5031	65.0693
24 × 24	68.7169	52.5059	65.1301
Ketabdari et al.[17]	69.1550	53.6150	-
Difference (%)	0.634	2.069	-

VALIDATION

According to the authors, no literature exists on using the modified Vlasov model to analyze the vibration of skew plates on elastic foundations. Therefore, due to a lack of valid data, the plate on the Vlasov foundation's vibration study findings was compared with rectangular results by setting a skew angle, β =90°.

Consider the problem for validation with the software Staad Pro. [37] A thin plate was used to validate the present formulation. Verification plate dimensions: (1 m × 1 m × 0.01 m, β = 60º) and plate material: Young's modulus E = 200 GPa, Poisson's ratio v = 0.3, and density, ρ = 7833.41 kg/m³; modulus of subgrade reaction (K) = 50 kPa/m, The calculated circular frequency of the present study (PS) and FE solution are presented in Table 2, which agrees with Staad Pro [37].

Table 2: Comparisons of the natural frequency parameter

Frequency parameter	CLAMPED (λ)			SS (λ)			FF (λ)		
	PS	FE solution [37]	Diff. (%)	PS	FE solution [37]	Diff. (%)	PS	FE solution [37]	Diff. (%)
λ_1	69.583	69.667	0.121	57.808	57.641	0.290	52.249	52.249	0.000
λ_2	96.848	96.948	0.104	74.042	73.826	0.292	52.249	52.249	0.000
λ_3	117.174	117.452	0.236	88.364	88.071	0.333	52.249	52.249	0.000
λ_4	130.239	130.238	0.001	98.567	98.135	0.440	53.503	53.487	0.030
λ_5	173.358	173.161	0.114	133.126	132.664	0.348	56.898	56.859	0.068
λ_6	173.384	173.702	0.183	133.281	133.024	0.193	58.647	58.512	0.230
λ_7	193.063	193.506	0.229	149.129	148.788	0.229	62.916	62.947	0.050
λ_8	224.998	224.469	0.236	176.979	176.030	0.539	68.043	67.818	0.332
λ_9	225.012	225.013	0.001	177.130	176.482	0.367	73.461	72.938	0.717

Gibigaye et al. [22] used a thin plate to validate the present formulation. Verification plate dimensions: (5 m × 3.5 m × 0.25 m) and plate material: Young's modulus E = 24000 MPa, Poisson's ratio v = 0.25, and density, ρ = 2500 kg/m³; soil E_s = 50 MPa, ν_s = 0.35, density,ρ_s = 1800 kg/m³, and H = 1.5 m, γ = 4.212. Frequency Parameter, $\tau_n = 4\omega_n a^2\sqrt{(\rho h+m_\circ)}/D$; The calculated frequency parameter is presented in Table 3, and the exact solution agrees with Gibigaye et al. [22]. For this case, the γ value is 4.212; hence, the other parameters were also validated.

Table 3: Comparisons of the natural frequency parameter

Reference	B.C	τ_1	τ_2	τ_3	τ_4	τ_5	τ_6	τ_7	τ_8	τ_9	τ_{10}
PS	FFFF	48.49	51.47	53.22	57.97	58.69	72.36	73.11	81.82	84.76	103.26
Gibigaye et al. [22]		48.69	52.00	53.47	58.97	59.20	72.97	73.57	80.81	86.29	103.71
PS	CCCC	73.45	102.07	144.60	154.58	174.57	226.31	229.92	262.40	292.34	300.10
Gibigaye et al. [22]		73.35	101.76	144.37	154.91	174.84	225.53	229.27	261.74	291.56	299.52
PS	SSSS	55.64	76.31	102.60	119.45	129.74	176.74	185.21	198.03	226.89	244.16
Exact		55.64	76.31	102.58	119.43	129.72	176.73	185.11	197.81	226.71	244.10
Gibigaye et al. [22]		55.46	76.48	102.95	119.67	129.55	176.89	185.08	197.93	226.81	244.19

The outcomes are also provided for a plate with multiple boundary conditions. In this instance, the results are also provided for a range of foundation coefficients, corresponding to a plate without an elastic foundation and a plate supported by an elastic foundation of the Winkler- or Pasternak-type. Tables 1, 2, and 3 provide the outcomes for the CCCC, SSSS, and FFFF plates using a 20 × 20 mesh. Comparisons between the reference and current results demonstrate the high degree of accuracy of the existing formulation.

RESULTS AND DISCUSSIONS

The dimensions of the plate were taken as follows for the parametric study for the parameters aspect ratio (a/b), depth of rigid base (H), skew angle (β), and vertical decay function(γ): a/b = 0.5, 1.0, and 2.0, and plate material characteristics Young's modulus, E = 200 GPa, Poisson's ratio, v = 0.3, density, ρ = 7850 kg/m³, β = 30º,45º,60º and H = 1 m, 3 m, 5 m, and 6 m; soil E_s = 50 MPa, 60 MPa, 75 MPa, and 90 MPa; Poisson's ratio, ν_s = 0.20, 0.25, and 0.30; density, ρ_s = 1700 kg/m³; and. γ = 1,2,3.

Frequency Parameter, $\tau_n = 4\omega_n a^2/\pi^2\sqrt{(\rho h+m_\circ)}/D$; results are presented in Table 4 – 6 and 7 - 12 in appendix-A, showing the variation of the first ten frequency parameters.

Table 4: Natural frequency parameter of skew plate, B.C.- CCCC, $\beta = 30^0$, $v_s = 0.20$, $\rho_s = 1700$ kg/m³ and $\gamma = 1$.

a/b	E_s (MN/m²)	H (m)	τ_1	τ_2	τ_3	τ_4	τ_5	τ_6	τ_7	τ_8	τ_9	τ_{10}
0.5	50	1.0	95.11	112.82	139.03	171.70	209.70	241.52	255.15	269.05	305.25	311.43
		3.0	109.24	133.84	168.22	208.23	250.99	262.43	293.04	297.62	341.26	350.00
		5.0	121.42	150.67	191.07	237.14	280.88	283.60	315.36	331.70	369.77	386.42
		6.0	126.91	158.06	201.00	249.75	289.51	297.56	326.14	346.21	383.68	402.28
	60	1.0	96.94	115.46	142.59	176.02	214.49	243.99	259.86	271.67	310.27	314.60
		3.0	113.19	139.33	175.65	217.58	261.57	268.19	299.91	308.69	349.95	361.72
		5.0	126.97	158.10	201.03	249.77	289.54	297.59	326.17	346.23	383.70	402.30
		6.0	133.14	166.29	211.98	263.69	299.47	312.67	338.90	361.93	400.05	419.75
	75	1.0	99.60	119.25	147.67	182.23	221.42	247.49	266.82	275.53	317.60	319.29
		3.0	118.76	146.94	185.92	230.54	276.18	276.52	309.98	323.95	362.81	378.02
		5.0	134.70	168.30	214.62	267.04	301.93	316.22	342.08	365.63	404.10	423.90
		6.0	141.78	177.55	226.91	282.67	313.64	332.53	357.69	382.82	423.80	443.41
	90	1.0	102.16	122.84	152.50	188.15	228.04	250.85	273.59	279.32	323.93	324.68
		3.0	123.98	153.95	195.34	242.47	284.51	289.49	319.82	337.80	375.47	393.02
		5.0	141.86	177.61	226.95	282.70	313.68	332.56	357.72	382.85	423.83	443.44
		6.0	149.75	187.80	240.41	299.82	327.02	349.82	376.00	401.39	446.44	464.76
1.0	50	1.0	163.71	244.58	319.71	329.78	399.81	455.40	483.22	570.50	574.17	577.10
		3.0	205.94	322.75	389.43	426.84	534.39	550.72	625.87	659.17	688.48	753.89
		5.0	240.86	381.13	438.73	505.01	625.64	633.31	695.12	767.74	780.96	884.09
		6.0	256.14	406.14	460.69	538.20	658.44	675.45	723.15	817.53	821.16	937.24
	60	1.0	171.27	255.91	334.23	337.88	417.24	467.43	502.68	582.92	584.84	598.77
		3.0	218.02	342.28	405.58	452.79	566.98	575.13	650.64	692.13	718.53	796.97
		5.0	256.58	406.42	460.93	538.41	658.61	675.62	723.31	817.66	821.30	937.36
		6.0	273.41	433.83	485.47	574.64	694.98	721.71	754.62	865.64	872.68	992.49
	75	1.0	181.79	271.60	349.44	354.38	441.60	484.54	529.87	595.82	605.36	629.50
		3.0	234.58	368.89	428.15	488.04	608.93	611.38	680.79	741.96	760.10	855.24
		5.0	278.02	440.70	491.69	583.48	703.89	732.83	762.35	876.36	885.92	1005.21
		6.0	296.93	471.31	519.70	623.71	745.03	784.13	798.39	926.09	947.57	1062.36
	90	1.0	191.51	286.02	360.41	372.95	464.19	500.70	554.87	608.63	624.83	658.34
		3.0	249.70	393.03	449.12	519.89	640.07	651.61	707.50	788.93	798.24	906.91
		5.0	297.50	471.67	520.03	623.99	745.26	784.34	798.60	926.28	947.75	1062.52
		6.0	318.25	505.11	551.15	667.74	790.67	839.03	840.22	980.72	1015.13	1122.67
2.0	50	1.0	382.34	453.24	556.99	685.37	835.08	975.75	1019.38	1086.89	1218.17	1249.32
		3.0	437.99	536.41	673.12	831.56	1001.49	1059.94	1180.52	1188.39	1366.06	1397.43
		5.0	486.05	603.22	764.30	947.30	1131.96	1133.32	1267.18	1326.51	1477.68	1543.44
		6.0	507.76	632.57	803.96	997.82	1165.66	1189.92	1308.97	1385.33	1532.30	1606.95
	60	1.0	389.56	463.68	571.13	702.68	854.40	986.37	1037.41	1097.17	1238.26	1261.73
		3.0	453.57	558.16	702.75	868.98	1044.20	1082.47	1207.24	1233.20	1400.08	1444.41
		5.0	507.98	632.75	804.10	997.94	1165.76	1190.02	1309.06	1385.41	1532.38	1607.02
		6.0	532.37	665.30	847.87	1053.76	1204.50	1251.27	1358.43	1448.86	1596.91	1676.81
	75	1.0	400.03	478.64	591.36	727.55	882.28	1000.84	1064.72	1112.29	1267.56	1280.12
		3.0	475.57	588.38	743.74	920.89	1103.27	1114.97	1246.32	1295.07	1450.39	1509.81
		5.0	538.54	673.31	858.46	1067.18	1214.07	1265.70	1370.81	1463.81	1612.95	1693.42
		6.0	566.53	710.12	907.63	1129.93	1259.78	1331.81	1431.67	1532.92	1691.20	1771.32
	90	1.0	410.12	492.87	610.56	751.23	908.95	1014.33	1091.65	1127.11	1295.90	1298.28
		3.0	496.19	616.27	781.37	968.66	1146.17	1157.17	1284.48	1351.23	1500.04	1569.90
		5.0	566.83	710.36	907.82	1130.08	1259.92	1331.93	1431.79	1533.03	1691.30	1771.41
		6.0	598.01	750.95	961.74	1198.85	1311.99	1401.47	1503.70	1607.21	1781.60	1856.49

Table 5: Natural frequency parameter of skew plate, B.C. - SSSS, $\beta = 30^0$, $v_s = 0.20$, $\rho_s = 1700$ kg/m³ and $\gamma = 1$.

a/b	E_s (MN/m²)	H (m)	τ_1	τ_2	τ_3	τ_4	τ_5	τ_6	τ_7	τ_8	τ_9	τ_{10}
0.5	50	1.0	54.08	70.54	93.34	119.65	147.44	158.76	178.61	180.16	213.08	215.39
		3.0	70.95	94.23	125.36	159.25	182.42	190.20	211.27	224.29	252.07	265.84
		5.0	84.53	112.13	149.08	188.43	203.45	219.08	241.30	256.30	288.38	302.97
		6.0	90.46	119.82	159.20	200.66	213.30	230.78	255.51	269.63	305.19	318.65
	60	1.0	56.51	73.76	97.49	124.62	152.85	161.48	183.52	184.28	217.24	221.46
		3.0	75.47	100.16	133.18	168.87	189.01	199.97	220.48	234.94	263.35	278.05
		5.0	90.54	119.87	159.25	200.70	213.34	230.81	255.54	269.65	305.22	318.67
		6.0	97.09	128.30	170.31	213.80	224.78	243.46	271.66	284.17	324.21	335.82
	75	1.0	59.95	78.26	103.30	131.61	160.46	165.45	188.48	192.31	223.39	230.10
		3.0	81.71	108.26	143.84	181.94	198.51	212.81	234.07	249.20	279.72	294.61
		5.0	98.75	130.38	172.99	216.90	227.63	246.49	275.57	287.64	328.79	339.90
		6.0	106.12	139.80	185.31	230.97	241.36	260.57	294.05	303.83	350.54	359.03
	90	1.0	63.18	82.45	108.71	138.14	167.54	169.30	193.37	199.80	229.46	238.25
		3.0	87.42	115.63	153.50	193.69	207.62	224.09	247.23	261.94	295.35	309.55
		5.0	106.22	139.88	185.36	231.02	241.40	260.61	294.08	303.87	350.57	359.06
		6.0	114.31	150.17	198.78	245.95	257.16	276.07	314.52	321.59	374.66	379.97
1.0	50	1.0	119.37	182.14	242.82	243.56	308.39	348.86	375.63	442.21	442.62	451.21
		3.0	161.57	259.09	307.72	347.78	441.08	447.34	508.14	543.88	564.22	629.43
		5.0	197.34	317.18	359.72	424.40	523.40	537.71	575.83	655.56	657.19	755.48
		6.0	212.89	342.03	382.58	456.91	556.46	578.80	604.94	697.22	704.44	805.50
	60	1.0	127.73	193.83	252.72	257.53	326.11	361.73	395.51	452.63	457.59	473.87
		3.0	174.17	278.66	324.96	373.32	472.27	473.03	530.93	579.64	594.65	671.69
		5.0	213.42	342.36	382.88	457.16	556.66	578.99	605.13	697.39	704.60	805.64
		6.0	230.44	369.55	408.24	492.62	593.18	623.89	637.64	741.36	758.31	857.23
	75	1.0	139.21	209.91	265.68	277.81	350.66	379.87	422.79	467.42	479.35	505.56
		3.0	191.30	305.26	348.83	407.96	506.64	516.46	561.18	630.14	636.44	728.08
		5.0	235.20	376.43	414.69	501.33	602.14	634.76	645.69	752.00	771.24	869.24
		6.0	254.19	406.71	443.38	540.68	643.27	682.92	684.68	801.12	831.20	923.79
	90	1.0	149.72	224.62	277.85	296.39	373.25	396.85	447.20	482.35	499.76	534.97
		3.0	206.83	329.34	370.80	439.23	538.13	555.75	588.81	674.57	676.56	777.21
		5.0	254.86	407.13	443.76	540.99	643.54	683.17	684.93	801.33	831.41	923.97
		6.0	275.59	440.14	475.40	583.76	688.76	724.67	739.28	854.95	896.81	982.49
2.0	50	1.0	216.50	282.56	373.54	478.24	589.20	640.57	713.95	726.20	855.50	860.30
		3.0	283.79	377.10	501.44	636.63	734.00	761.52	848.00	897.65	1009.27	1061.91
		5.0	337.99	448.61	596.35	753.65	816.84	878.36	965.66	1026.46	1152.85	1210.35
		6.0	361.66	479.32	636.85	802.83	855.60	925.35	1021.83	1079.88	1219.63	1273.07
	60	1.0	226.23	295.39	390.11	498.10	610.93	651.34	736.68	739.41	871.92	884.53
		3.0	301.84	400.79	532.71	675.17	760.02	801.11	883.97	940.58	1053.79	1110.72
		5.0	361.97	479.56	637.03	802.98	855.73	925.47	1021.94	1079.98	1219.72	1273.16
		6.0	388.10	513.25	681.35	855.75	900.70	976.05	1085.96	1138.06	1295.28	1341.71
	75	1.0	239.95	313.36	413.33	526.08	641.52	667.04	758.91	768.88	896.21	919.07
		3.0	326.72	433.16	575.35	727.59	797.43	853.08	937.21	997.94	1118.53	1176.93
		5.0	394.74	521.56	692.06	868.21	911.92	988.12	1101.53	1151.91	1313.57	1358.03
		6.0	424.13	559.21	741.42	924.79	966.11	1044.17	1175.21	1216.53	1400.30	1434.51
	90	1.0	252.80	330.06	434.91	552.20	669.99	682.27	778.08	798.98	920.16	951.65
		3.0	349.52	462.61	614.03	774.78	833.28	898.52	989.06	1049.09	1180.53	1236.67
		5.0	424.53	559.51	741.65	924.98	966.28	1044.33	1175.35	1216.67	1400.42	1434.63
		6.0	456.80	600.67	795.44	984.64	1028.89	1105.69	1257.05	1287.32	1496.66	1518.26

Table 6: Natural frequency parameter of skew plate, B.C.- FFFF, $\beta = 30^0$, $v_s = 0.20$, $\rho_s = 1700$ kg/m³ and $\gamma = 1$.

a/b	E_s (MN/m²)	H (m)	τ_1	τ_2	τ_3	τ_4	τ_5	τ_6	τ_7	τ_8	τ_9	τ_{10}
0.5	50	1.0	28.19	37.38	49.39	53.29	62.77	63.23	77.37	78.18	93.28	94.68
		3.0	29.07	45.49	66.84	69.31	85.17	89.90	107.98	113.85	130.69	138.24
		5.0	30.89	52.28	80.08	81.98	101.03	109.70	129.39	139.93	156.82	169.86
		6.0	31.76	55.27	85.76	87.50	107.76	118.10	138.38	150.93	167.95	183.00
	60	1.0	30.65	40.59	53.70	57.97	68.16	68.44	83.76	84.16	100.59	101.31
		3.0	31.63	49.35	72.62	75.25	91.97	97.67	116.47	123.54	140.66	149.71
		5.0	33.61	56.70	86.95	88.98	109.04	119.13	139.53	151.84	169.08	183.87
		6.0	34.55	59.94	93.10	94.96	116.30	128.23	149.22	163.75	181.18	197.88
	75	1.0	33.94	44.89	59.47	64.23	75.40	75.43	92.24	92.42	110.36	110.55
		3.0	35.10	54.54	80.36	83.21	101.03	108.10	127.80	136.57	154.08	165.12
		5.0	37.29	62.66	96.16	98.37	119.74	131.78	153.04	167.79	185.56	202.07
		6.0	38.32	66.23	102.94	104.99	127.72	141.80	163.66	180.90	198.97	215.91
	90	1.0	36.90	48.74	64.64	69.81	81.60	81.98	99.50	100.24	118.58	119.57
		3.0	38.22	59.20	87.29	90.32	109.09	117.45	137.86	148.25	166.13	178.88
		5.0	40.60	68.00	104.40	106.78	129.29	143.09	165.05	182.05	200.35	217.05
		6.0	41.72	71.87	111.74	113.97	137.93	153.93	176.50	196.21	214.93	232.13
1.0	50	1.0	89.07	124.93	143.87	158.65	192.87	196.24	226.15	235.75	241.48	275.92
		3.0	89.35	151.20	168.47	209.36	251.71	276.54	290.68	320.66	349.14	392.41
		5.0	94.26	174.55	192.51	248.29	299.63	336.06	339.64	383.85	428.86	469.19
		6.0	96.61	184.86	203.50	264.93	320.62	361.14	361.34	410.70	462.53	501.86
	60	1.0	96.85	135.91	155.19	172.59	208.88	213.50	242.35	254.86	260.95	298.61
		3.0	97.38	164.76	182.05	227.57	273.08	300.88	311.00	346.87	379.41	422.24
		5.0	102.74	190.14	208.46	269.59	325.33	364.58	365.35	415.10	465.87	505.43
		6.0	105.30	201.31	220.52	287.55	348.21	388.17	392.70	444.09	502.30	541.02
	75	1.0	107.38	150.69	170.20	191.32	230.26	236.76	263.45	280.49	287.85	329.01
		3.0	108.27	183.03	200.37	251.99	301.78	333.56	338.39	381.87	420.12	462.07
		5.0	114.23	211.10	230.04	298.12	359.89	398.37	404.59	456.79	515.43	554.21
		6.0	117.04	223.40	243.57	317.85	385.30	424.81	434.69	488.65	555.48	593.75
	90	1.0	116.90	163.97	183.53	208.12	249.32	257.67	281.97	303.40	312.38	356.03
		3.0	118.10	199.47	216.90	273.85	327.51	362.85	363.09	413.04	456.61	497.70
		5.0	124.59	229.90	249.55	323.65	390.90	428.93	439.67	493.94	559.67	598.02
		6.0	127.63	243.19	264.40	344.95	418.57	457.94	472.19	528.38	602.92	641.13
2.0	50	1.0	451.17	598.15	790.25	852.93	1004.24	1012.10	1237.81	1250.72	1492.34	1513.69
		3.0	465.12	727.92	1069.65	1109.48	1363.53	1438.93	1727.74	1822.39	2090.53	2212.96
		5.0	494.25	836.68	1281.62	1312.19	1617.58	1756.39	2070.39	2240.85	2509.12	2720.49
		6.0	508.22	884.52	1372.61	1400.41	1725.23	1891.19	2214.45	2417.44	2687.15	2931.27
	60	1.0	490.43	649.59	859.11	928.03	1090.52	1095.51	1340.11	1346.40	1609.43	1619.82
		3.0	506.16	789.71	1162.09	1204.61	1472.44	1563.42	1863.67	1977.77	2250.22	2397.06
		5.0	537.80	907.47	1391.73	1424.15	1745.76	1907.77	2232.81	2431.98	2705.25	2945.19
		6.0	552.89	959.30	1490.30	1519.82	1861.89	2053.84	2387.96	2623.31	2898.79	3164.87
	75	1.0	543.16	718.45	951.54	1028.31	1206.96	1207.00	1475.73	1478.79	1764.79	1768.84
		3.0	561.62	872.79	1286.09	1331.91	1617.51	1730.69	2044.94	2186.77	2465.16	2644.23
		5.0	596.64	1002.72	1539.36	1574.24	1916.93	2110.75	2449.04	2688.20	2968.89	3231.92
		6.0	613.24	1059.91	1648.02	1679.97	2044.63	2271.74	2619.05	2898.96	3183.26	3452.90
	90	1.0	590.49	780.04	1034.29	1117.60	1306.29	1311.71	1591.96	1604.05	1896.40	1913.38
		3.0	611.65	947.41	1397.09	1445.68	1746.61	1880.58	2206.10	2374.18	2658.03	2864.97
		5.0	649.71	1088.28	1671.43	1708.60	2069.74	2292.26	2641.28	2917.19	3205.36	3471.22
		6.0	667.64	1150.24	1789.09	1823.38	2207.94	2466.45	2824.67	3145.04	3438.41	3712.10

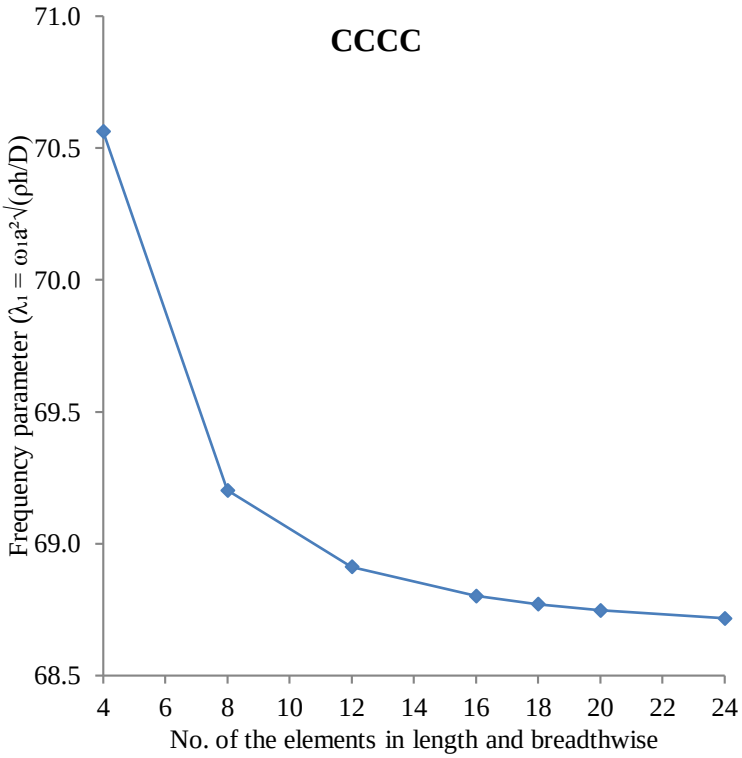

Fig. 5 First mode convergence study for a clamped plate's natural frequency

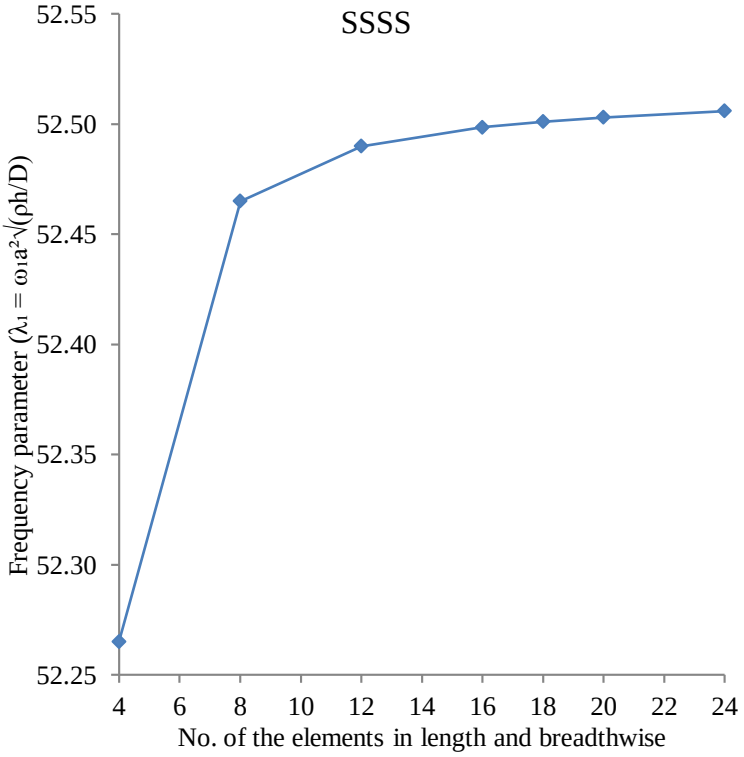

Fig. 6 First mode convergence study for a simply supported plate natural frequency

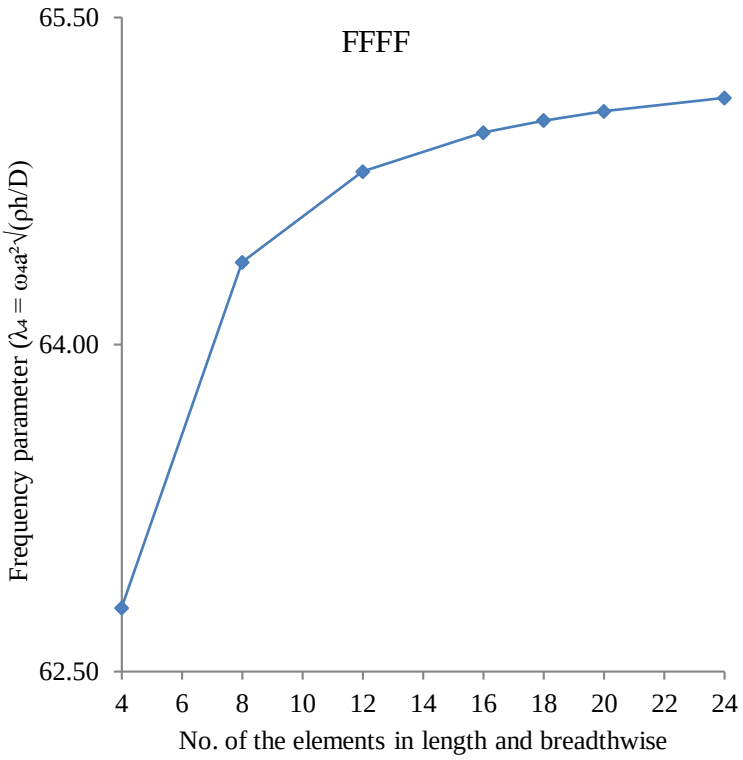

Fig. 7 Fourth mode convergence study for a free plate natural frequency

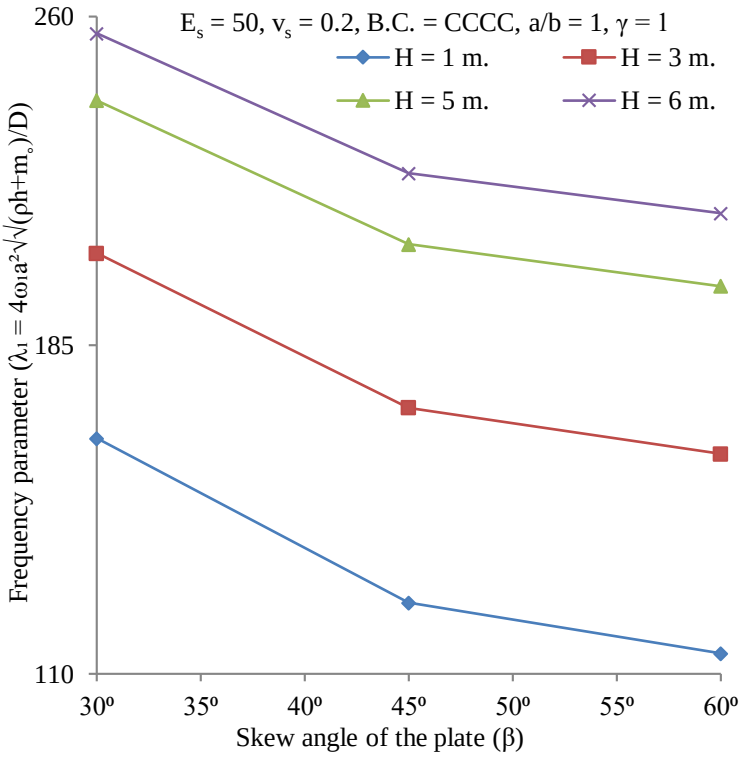

Fig. 8 Variation of frequency parameter of CCCC plate with the skew angle of the plate

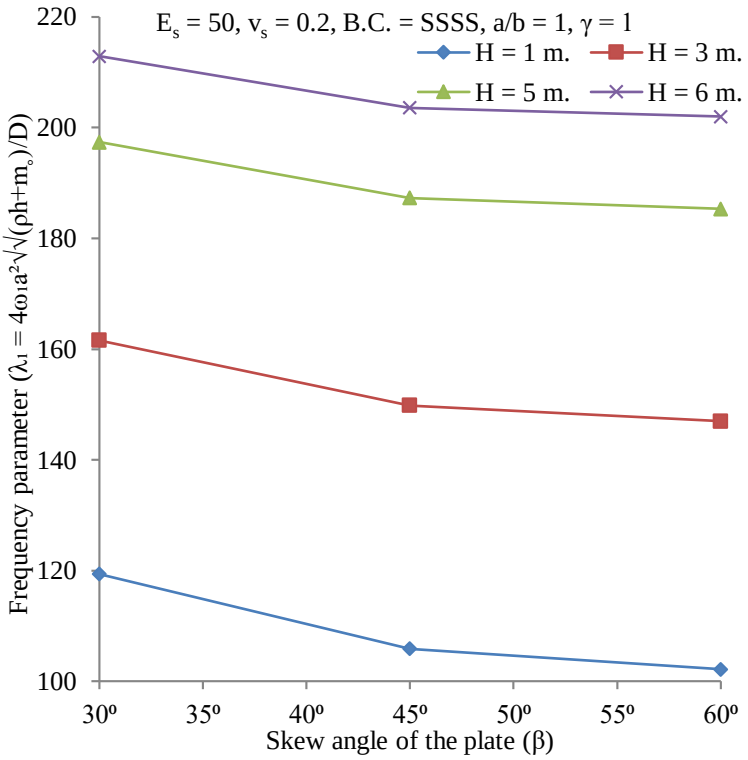

Fig. 9 Variation of frequency parameter of SSSS plate with the skew angle of the plate

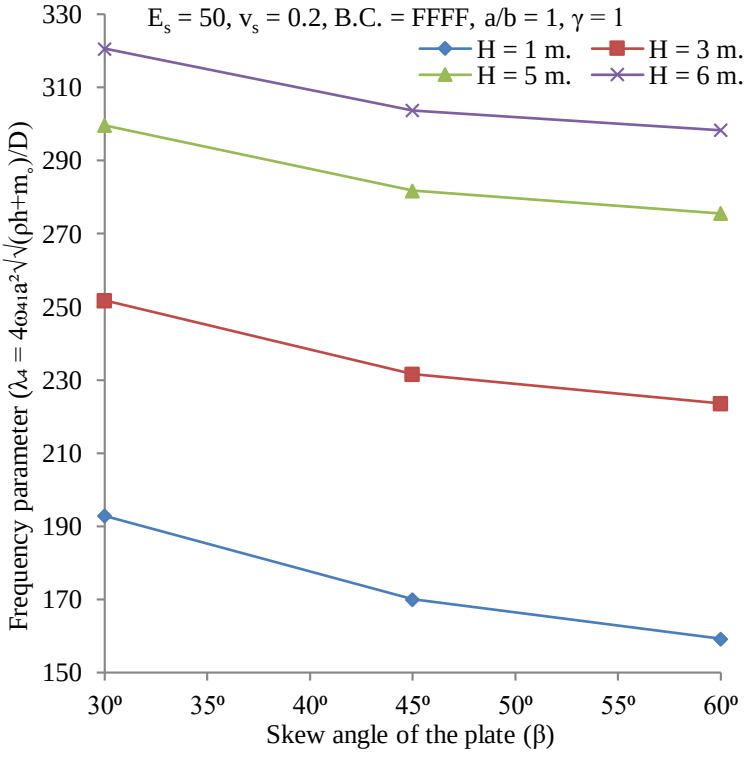

Fig. 10 Variation of frequency parameter of FFFF plate with the skew angle of the plate

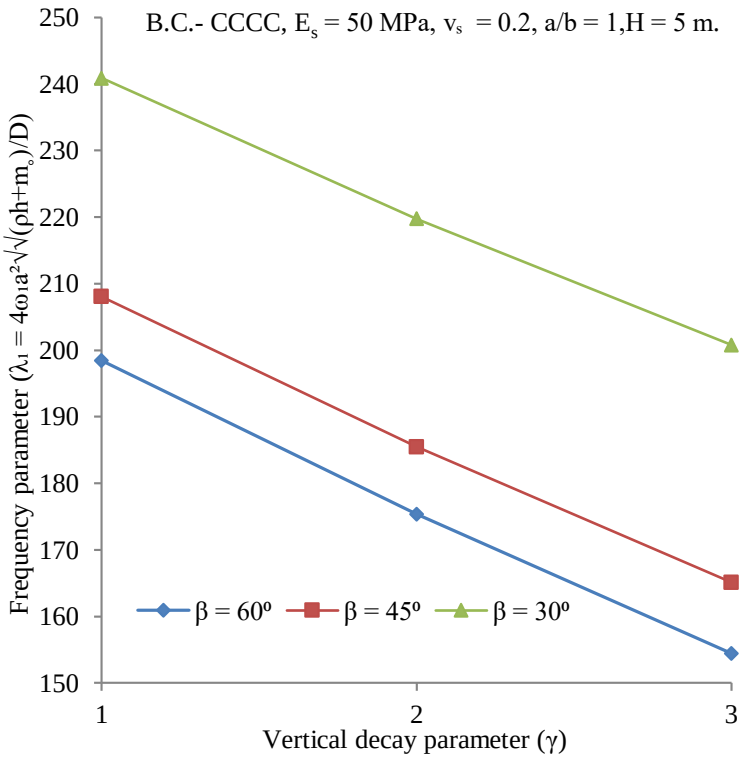

Fig. 11 Variation of frequency parameter of CCCC plate with the vertical decay parameter (γ)

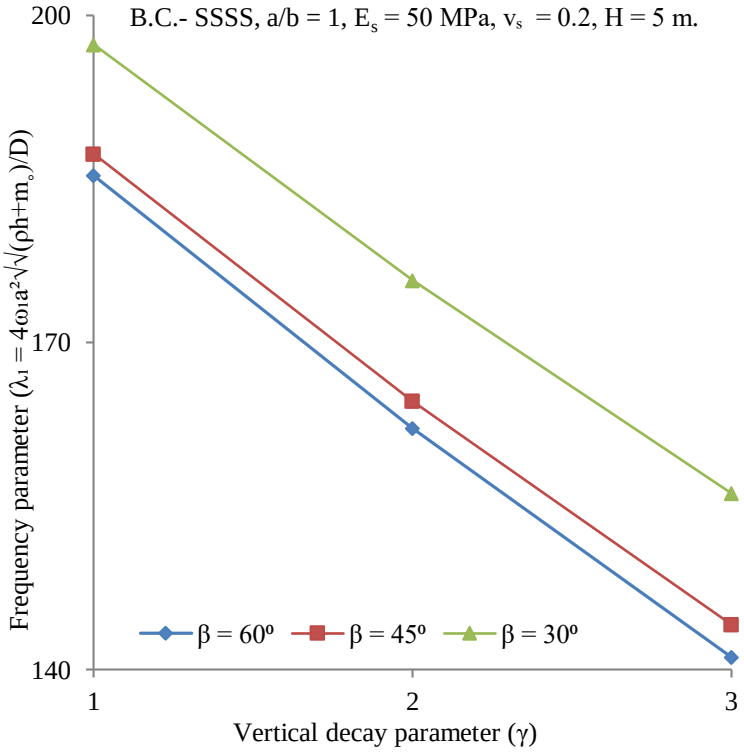

Fig. 12 Variation of frequency parameter of SSSS plate with the vertical decay parameter (γ)

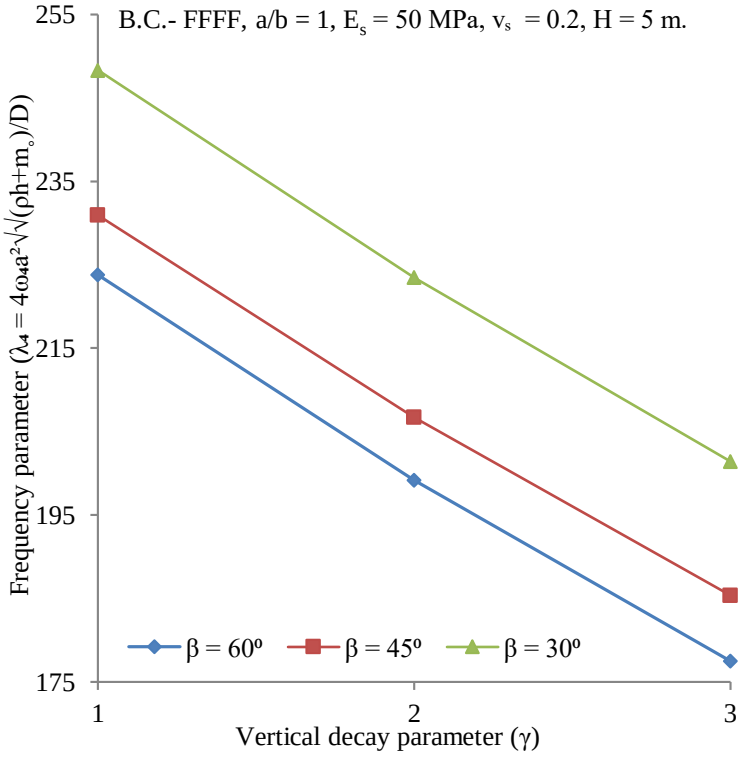

Fig. 13 Variation of frequency parameter of FFFF plate with the vertical decay parameter (γ)

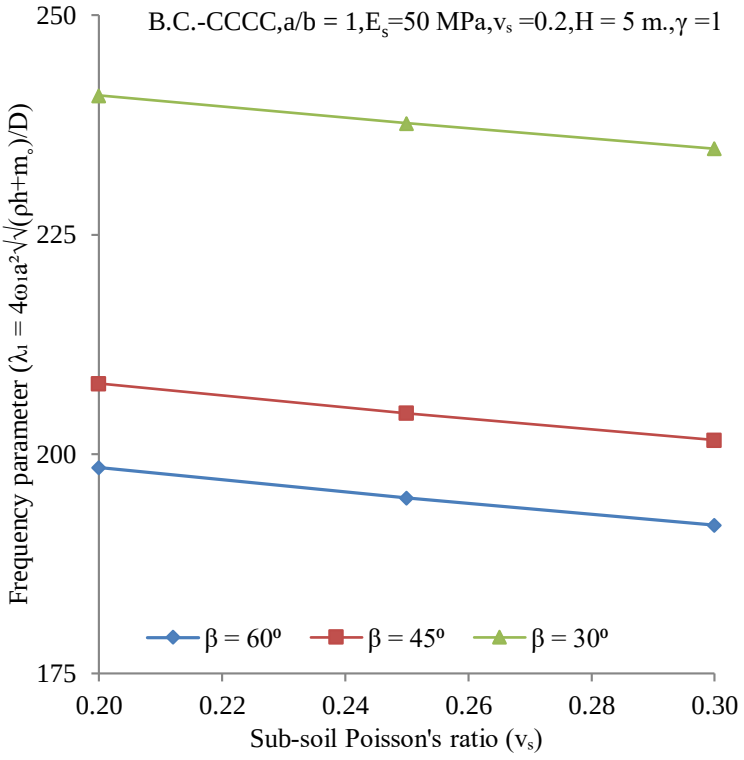

Fig. 14 Variation of frequency parameter of CCCC plate with the sub-soil Poisson's ratio (v_s)

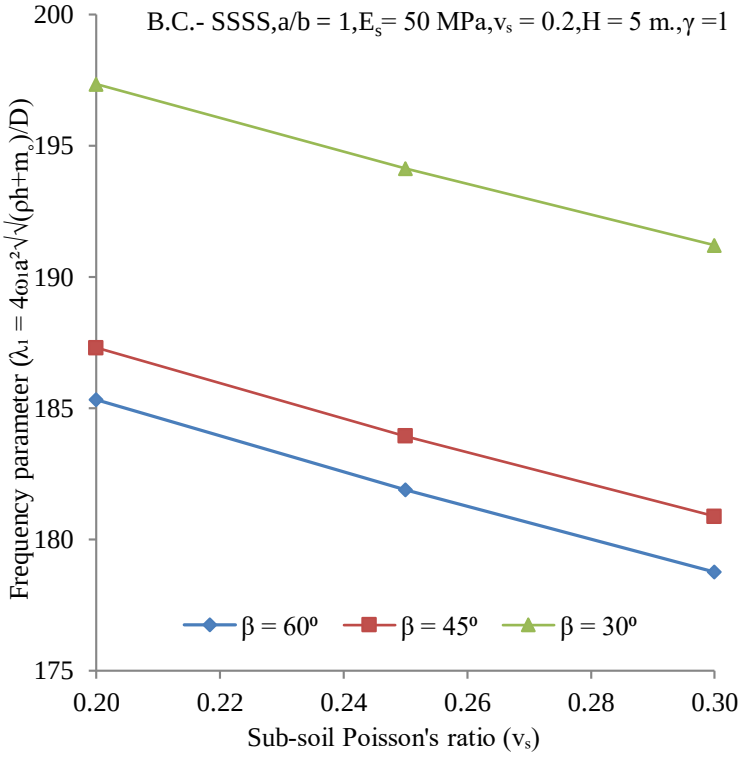

Fig. 15 Variation of frequency parameter of SSSS plate with the sub-soil Poisson's ratio (v_s)

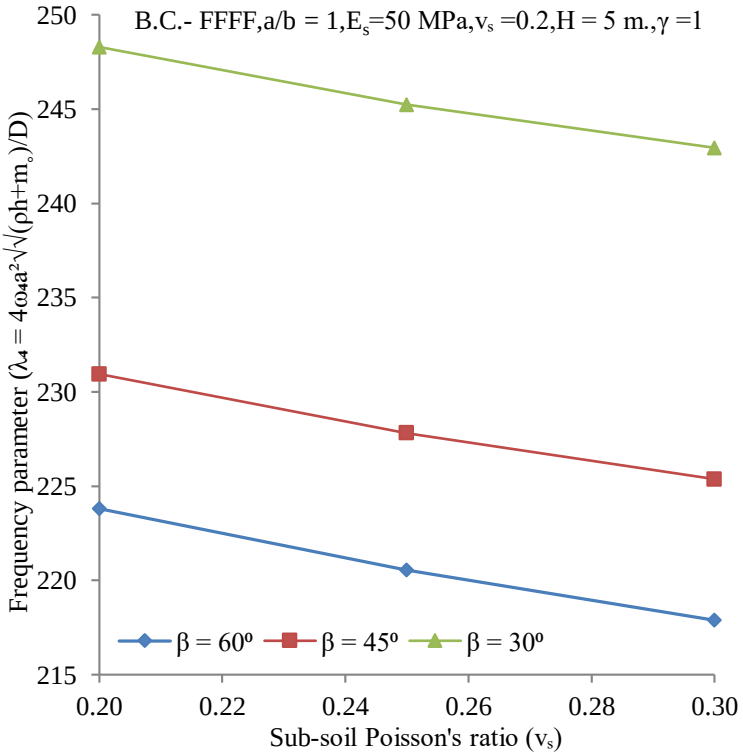

Fig. 16 Variation of frequency parameter of FFFF plate with sub-soil Poisson's ratio (v_s)

In this study, the mode shapes of the plate on an elastic foundation are also obtained for all parameters considered. Since the presentation of these entire mode shapes would take up excessive space, only the ten-mode shapes of the plate for $\gamma = 2$, $H = 5$, $\beta = 60^o$and b/a= 1 are presented. These mode shapes are given in Fig. 17. As seen from the figures, the number of half-waves increases as the mode increases. It is seen that the shapes of eigenmodes reveal the real physical modes.

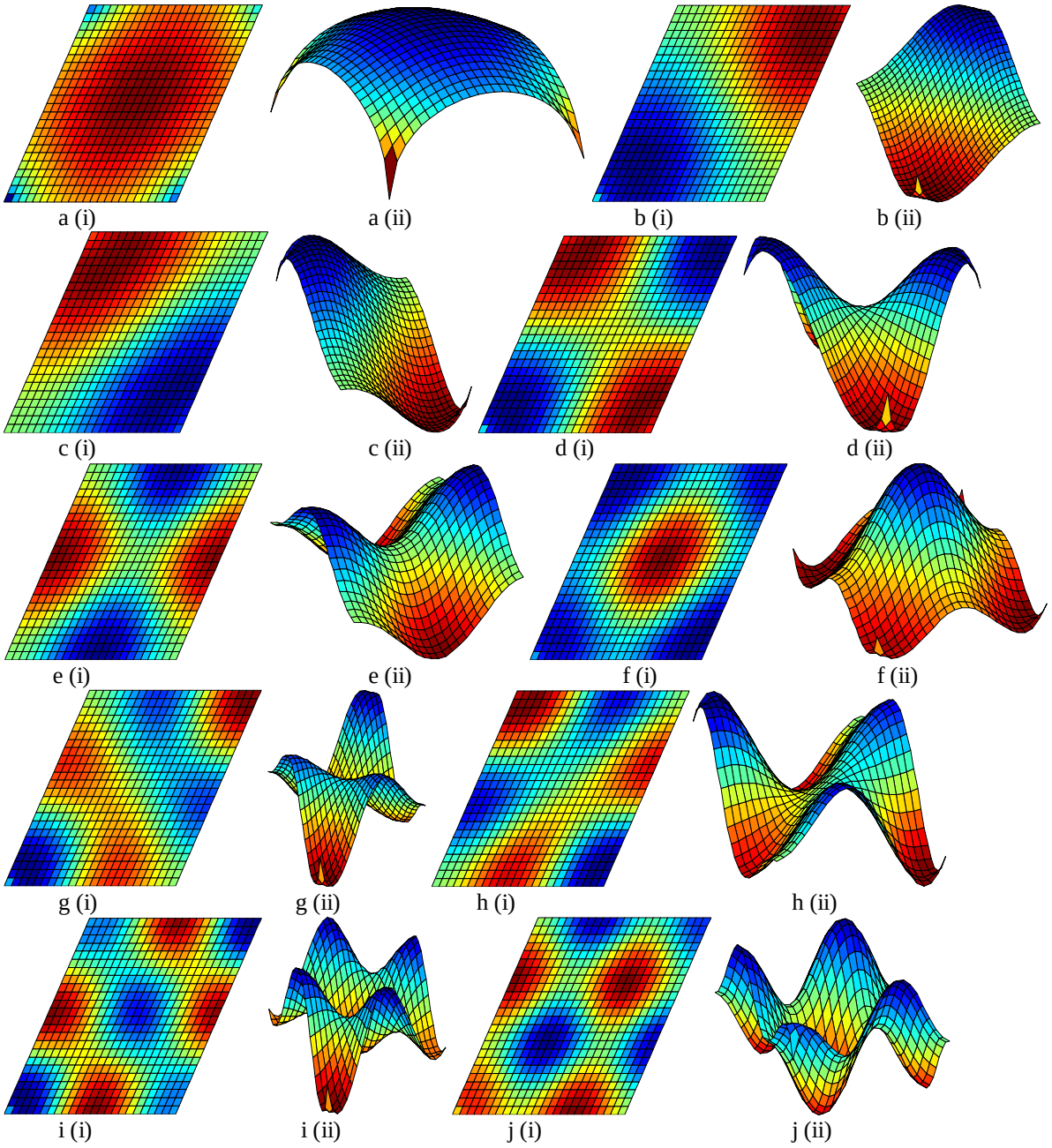

Fig. 17 First ten-mode shapes of the plate on elastic foundations for $\gamma = 2$, $H = 5$, $\beta = 60^{o}$ and $b/a = 1$ (a) The first mode shape; (b) The second mode shape; (c) The third mode shape; (d) The fourth mode shape; (e) The fifth mode shape; (f) The sixth mode shape; (g) The seventh mode shape; (h) The eight mode shape; (i) The ninth mode shape; (j) The tenth mode shape.

The relation between frequency parameters and the skew angle is illustrated in Figure 8, which demonstrates that the frequency parameter decreases as the skew angle increases for the CCCC plate; Figure 9 indicates that the skew angle has little effect on the frequency parameter for the SSSS plate and Figure 10 suggests that the skew angle having a negligible impact on the frequency parameter for the FFFF plate, as the edge constraints increase, the effect of the skew angle increases. Figures 11 through 13 illustrate the relationship between the frequency and vertical decay parameters (γ). Figure 11 indicates a linear decline in the frequency parameter whenever there is a rise in the vertical decay parameter for the CCCC plate. Figure 12 demonstrates a linear decrease in the frequency parameter whenever there is a rise in the vertical decay parameter for the SSSS plate. Figure 13 indicates a linear decline in the frequency parameter whenever there is a rise in the vertical decay parameter for the FFFF plate. Figure 14 indicates the Poisson's ratio of the subsoil has a negligible impact on the frequency parameter for the CCCC plate. Figure 15 shows the Poisson's ratio of the subsoil has little

effect on the frequency parameter for the SSSS plate, and Figure 16 indicates the Poisson's ratio of the subsoil has a negligible impact on the frequency parameter for the FFFF plate. In addition, it has been discovered that the frequency parameter also rises as the edge constraints get more stringent. As a result, this reveals that edge restrictions that are bigger than average improve the flexural stiffness of the plate and, as a consequence, its frequency response. In addition, it has been observed that the value of the active mass, m_0, and the second fundamental parameter, G_b, decreases as the value increases. On the other hand, the first essential parameter, also known as the Winkler parameter, K, rises when the value increases. It has been observed, without respect to boundary conditions or other factors, that the frequency parameter of the plate increases as the aspect ratio does. This is the case regardless of any additional parameters. It can be shown that the plate's frequency parameter increases linearly with the sub-soil elastic modulus, Es, independent of the boundary conditions and any other parameters that may be present. Although boundary conditions and other features are present, it can be observed that the frequency parameter of the plate increases as the subsurface depth, H, increases. It is observed that the frequency parameter increases with the increase of the vertical decay function up to a b/H ratio of 2.5 and then decreases with the rise of the vertical decay function. It is observed that the first foundation parameter, K, increases with an increase of **γ,** and the second foundation parameter, G_b, and activated mass, m_0, decreases with a rise in **γ.**

These findings suggest that variations in the other factors taken into account in this study always have a less substantial impact on the frequency characteristics of the skew plate on an elastic foundation than do changes in the subsoil depth. The frequency parameters with a constant value of H and γ fall as the b/a ratio grows, as Tables and Figures show. As the value of H rises, the frequency parameter values for constant values of b/a and γ drop. As the H/b ratio rises, the frequency parameter values with a constant value of H and γ increase. This behaviour makes sense for a skew plate on an elastic foundation since it becomes more flexible and has smaller frequency characteristics as the subsoil depth increases. Note that with a constant value of H and γ, the frequency parameters decrease with rising b/a ratios; this decline grows stronger for larger values of the frequency parameters.

CONCLUSIONS

This research uses a modified version of the Vlasov model and higher-order finite elements to conduct a free vibration analysis of plates resting on two-parameter elastic foundation supports. The results of using higher-order finite elements have a remarkable agreement with the precise solution and reference result, in addition to having a speedy convergence independent of the boundary conditions, aspect ratio, and foundation parameters. The shear parameter of the foundation has less impact on the plate's natural frequency than the foundation's Winkler parameter. Higher-order finite elements also provide an accurate approximation solution to the problem. The presently available higher-order finite elements for vibration analysis perform well for skew and rectangular thin plates resting on elastic foundations and provide a highly accurate approximation solution according to various numerical tests that include varied support conditions. Their provenance demonstrates that they generate an exact approximation solution. Important conclusions from this study are summarized below.

- ✓ The present formulation is simple, has rapid convergence, and performs efficiently and reliably exceptionally well for a thin, skewed plate on a two-parameter foundation with only a few elements. It saves computer memory and reduces computational cost, resources, and time.
- ✓ The only inputs are the modulus of elasticity, Poisson's ratio, and the thickness of the subsoil to represent the elastic foundation.
- ✓ Numerical results for skew plates and various support conditions will demonstrate the effectiveness of the present elements. Still, they will be a convenient reference for future academics, practitioners, and design engineers due to their ease of formulation, capacity to produce an approximate solution, and cost-effectiveness.
- ✓ Using the modified Vlasov model, the present element for vibration analysis of a skew plate on a two-parameter foundation overcomes the non-conformity of a four-nodded twelve degrees of freedom element.

REFERENCES

1. Hetenyi, M. (1950). “A General Solution for the Bending on an Elastic Foundation of Arbitrary Continuity”, *J Appl Phys, Vol. 21, pp. 55–58.*

2. Filonenko-Borodich, M.M. (1940). "Some Approximate Theories of Elastic Foundation", *Uch Zapi Mosk Gos, Univ Mekh, Vol. 46, pp. 3–18*.
3. Pasternak, P.L. (1954). "On a New Method of Analysis of an Elastic Foundation by Means of Two Foundation Constants", *Gos Izd Lit po Stroit Arkhitekture, Moscow*.
4. Morley, L.S.D. (1963). "Skew Plates and Strucrures", *Pergamon Press, Oxford*.
5. Butalia, T.S., Kant, T. and Dixit, V.D.T. (1990). "Performance of Heterosis Element For Bending of Skew Rhombic Plates", *Vol. 34, pp. 23–49*.
6. Sengupta, D. (1995). "Performance Study of A Simple Finite Element In The Analysis of Skew Rhombic Plates", *Comput Struct,Vol. 54, pp. 1173–82*.
7. Sengupta, D. (1991). "Stress Analysis of Flat Plates With Shear Using Explicit Stiffness Matrix", *Int J Numer Methods Eng, Vol. 32, pp. 1389–1409*.
8. Sengupta, D. (1993). "Direct Computation of Moment, Shear and Reaction in Flat Plates Using a triangular Element Free from Locking", *Compurers Struct,Vol. 48, pp. 843–50*.
9. Srinivasa, C.V., Suresh, Y.J., Kumar, W.P.P. and Banagar, A.R. (2018). "Bending Behavior of Simply Supported Skew Plates", *Int J Sci Eng Res, Vol. 9, pp. 21–26*.
10. Liew, B.K.M. and Han, J.-B. (1997). "Bending Analysis of Simply Supported Shear Deformable Skew Plates", *pp. 214–221*.
11. Chun, P. and Lim, Y.M. (2011). "Analytical Behavior Prediction for Skewed Thick Plates on Elastic Foundation", *https://doi.org/10.1155/2011/509724*.
12. Chun, P. and Ohga, M. (2012). "Analytical Method to Predict the Bending Behavior of Skewed Thick Plates on Winkler Foundation", *J Japan Soc Civ Eng Ser A2 (Applied Mech), Vol. 68, pp. 33–43, https://doi.org/10.2208/iscejam.68.I*.
13. Xenalevina, Sidara, S.C. and Maknun, I.J. (2020). "Convergence Behavior of DKMQ Element in Functionally Graded Material (FGM) Skew Plate", *AIP Conf Proc, pp. 2296, https://doi.org/10.1063/5.0030634*.
14. Hassan, A.H.A. and Kurgan, N. (2020). "Bending Analysis of Thin FGM Skew Plate Resting on Winkler Elastic Foundation Using Multi-Term Extended Kantorovich Method", *Eng Sci Technol an Int J, Vol. 23, pp. 1–13, https://doi.org/10.1016/j.jestch.2020.03.009*.
15. Wang, X. and Yuan, Z. (2018). "Buckling Analysis of Isotropic Skew Plates Under General In-Plane Loads by the Modified Differential Quadrature Method", *Appl Math Model, Vol. 56, pp. 83–95, https://doi.org/10.1016/j.apm.2017.11.031*.
16. Joodaky, A. and Joodaky, I. (2015). "A Semi-Analytical Study on Static Behavior of Thin Skew Plates on Winkler And Pasternak Foundation", *Int J Mech Sci, Vol. 100, pp. 322–327. https://doi.org/10.1016/j.ijmecsci.2015.06.025*.
17. Ketabdari, M.J., Allahverdi, A., Boreyri, S. and Ardestani, M.F. (2016). "Free Vibration Analysis of Homogeneous and FGM Skew Plates Resting on Variable Winkler-Pasternak Elastic Foundation", *Mech Ind, Vol. 17, https://doi.org/10.1051/meca/2015051*.
18. Vallabhan, C.V.G. and Das, Y.C. (1988). "Parametric Study of Beams on Elastic Foundations", *J Eng Mech Div ASCE, Vol. 114, pp. 2072–82*.
19. Özgan K. and Daloğlu, A.T. (2012). "Free Vibration Analysis of Thick Plates on Elastic Foundations Using Modified Vlasov Model with Higher Order Finite Elements", *Indian J Eng Mater Sci, Vol. 19, pp. 279–291*.
20. Hamarat, M.A., Çalık,Karaköse, ÜH. and Orakdöğen, E. (2012). "Seismic Analysis of Structures Resting on Two Parameter Elastic Foundation", *15th World Conf Earthq Eng*.
21. Buczkowski, R., Taczała, M. and Kleiber, M. (2015). "A 16-Node Locking-Free Mindlin Plate Resting on Two-Parameter Elastic Foundation – Static and Eigenvalue Analysis", *Comput Assist Methods Eng Sci, Vol. 22, pp. 99–114*.
22. Gibigaye, M., Yabi, C.P. and Degan, G. (2018). "Free Vibration Analysis of Dowelled Rectangular Isotropic Thin Plate on a Modified Vlasov Soil Type by Using Discrete Singular Convolution Method", *Appl Math Model, Vol. 61, pp. 618–633, https://doi.org/10.1016/j.apm.2018.05.019*.
23. Dutta, A.K., Mandal, J.J. and Bandyopadhyay, D. (2021). "Free Vibration Analysis of Beams on Elastic Foundation Using Quintic Displacement Functions", ISET J Earthq Technol, Vol. 58, pp. 45–59.

24. Bogner, F.K., Fox, R.L. and Schmit, L.A. (1966). "The Generation of Inter-Element-Compatible Stiffness and Mass Matrices by the Use of Interpolation Formulas", *In Proceedings of the Conference on Matrix Methods in Structural Mechanics, pp 397–444*.
25. Inc. M (2011). "The Language of Technical Computing MATLAB 2011b".
26. Selvaduari, A. (1979). "Elastic analysis of Soil-Foundation Interaction", *Amsterdam, Elsevier*.
27. Vlasov, V.Z. and Leont'ev, U.N. (1966). "Beams, Plates and Shells on Elastic Foundations", *Israel Progr Sci Transl, pp. 357*.
28. Turhan, A. (1992). "A Consistent Vlasov Model for Analysis of Plates on Elastic Foundations Using the Finite Element Method", *Ph.D. Dissertation, Texas Tech University, USA.*
29. Celik, M. and Saygun, A. (1999). "Method for the Analysis of Plates on a Two-Parameter Foundation", *Int J Solids Struct, Vol. 36, pp. 2891–15*.
30. Straughan, W. (1990). "Analysis of Plates on Elastic Foundation", *A Diss Civ Eng Grad Sch Texas Tech Univ Partial Fulfillment Requir Degree Dr Philos*.
31. Özgan, K. and Daloğlu, A.T. (2008). "Effect of Transverse Shear Strains on Plates Resting on elastic foundation Using Modified Vlasov Model", *Thin-Walled Struct, Vol. 46, pp. 1236–1250, https://doi.org/10.1016/j.tws.2008.02.006*.
32. Ozgan, K. and Daloglu, A.T. (2009). "Application of the Modified Vlasov Model to the Free Vibration Analysis of Thick Plates Resting on Elastic Foundations", *Shock Vib, Vol. 16, pp. 439–454, https://doi.org/10.3233/SAV-2009-0479*.
33. Petyt, M. (1990). "Introduction to Finite Element Vibration Analysis", *Cambridge University Press, Cambridge*.
34. Hinton, E. (1988). "Numerical Methods and Software for Dynamic Analysis of Plates and Shells", *Pineridge Press, Swansea*.
35. Dutta, A.K., Bandyopadhyay, D. and Mandal, J.J. (2021). "Free Vibration Analysis of Second-Order Continuity Plate Element Resting on Pasternak Type Foundation Using Finite Element Method", *Int J Pavement Res Technol, https://doi.org/10.1007/s42947-021-00099-x.*
36. Rao, S.S. (2007). "Vibration of Continuous Systems", *John Wiley & Sons, Inc*.
37. STAAD Pro. V8i (2014) – Structural Analysis Software from Bentley.

APPENDIX-A

Table 7: Natural frequency parameter of skew plate, B.C.- CCCC, $\beta = 45^0$, $v_s = 0.20$, $\rho_s = 1700$ kg/m³ and $\gamma = 1$

a/b	E_s (MN/m²)	H (m)	τ_1	τ_2	τ_3	τ_4	τ_5	τ_6	τ_7	τ_8	τ_9	τ_{10}
0.5	50	1.0	61.11	74.85	95.36	120.57	142.45	146.00	158.81	169.34	188.25	197.71
		3.0	78.61	98.48	126.56	159.31	169.96	182.88	198.76	207.87	237.50	241.16
		5.0	92.77	116.61	149.88	187.87	193.59	209.21	232.83	237.28	274.62	277.40
		6.0	98.98	124.47	159.92	199.86	204.51	220.76	247.73	250.20	289.27	294.86
	60	1.0	63.56	78.02	99.41	125.45	145.65	150.98	163.06	174.17	193.79	203.00
		3.0	83.29	104.45	134.22	168.71	177.44	191.43	209.73	217.37	250.35	251.96
		5.0	99.05	124.53	159.97	199.90	204.54	220.79	247.76	250.23	289.29	294.89
		6.0	105.93	133.21	171.02	212.77	217.14	233.66	264.24	264.61	305.56	314.22
	75	1.0	67.02	82.47	105.07	132.32	150.30	157.79	169.43	180.91	201.91	210.46
		3.0	89.77	112.66	144.70	181.51	188.09	203.23	225.02	230.55	266.94	268.22
		5.0	107.66	135.35	173.71	215.82	220.25	236.78	268.08	268.19	309.47	318.85
		6.0	115.44	145.12	186.13	229.87	235.07	251.46	284.42	286.73	327.90	340.64
	90	1.0	70.29	86.62	110.34	138.72	154.80	163.92	175.78	187.18	209.77	217.47
		3.0	95.73	120.16	154.26	193.03	198.22	214.11	239.10	242.73	280.76	284.69
		5.0	115.53	145.20	186.18	229.92	235.11	251.50	284.46	286.77	327.94	340.68
		6.0	124.10	155.95	199.82	245.24	251.70	267.78	302.56	307.14	348.31	364.64
1.0	50	1.0	126.16	190.74	217.75	250.80	312.75	316.82	343.01	388.10	391.51	451.57
		3.0	170.70	270.47	288.91	356.78	417.48	434.70	451.37	515.31	547.12	591.25
		5.0	208.02	330.72	345.67	433.89	498.01	509.46	549.51	607.46	664.12	690.12
		6.0	224.27	356.61	370.49	466.70	533.01	542.72	591.39	646.99	714.09	733.45
	60	1.0	134.64	202.68	228.00	265.64	326.58	334.75	354.81	407.53	408.48	471.85
		3.0	183.74	290.68	307.77	382.46	443.90	458.92	483.77	545.61	585.56	623.38
		5.0	224.77	356.93	370.80	466.94	533.22	542.93	591.58	647.16	714.25	733.61
		6.0	242.60	385.32	398.25	502.84	571.90	580.07	637.46	690.63	769.02	781.80
	75	1.0	146.31	219.10	242.40	286.08	345.98	359.58	371.54	429.99	437.00	498.49
		3.0	201.50	318.22	333.77	417.30	480.27	492.79	527.86	587.03	637.99	667.80
		5.0	247.52	392.49	405.20	511.66	581.38	589.24	648.58	701.19	782.20	793.51
		6.0	267.47	424.25	436.16	551.71	624.98	631.58	699.84	749.98	843.35	848.24
	90	1.0	157.00	234.14	255.84	304.78	364.07	382.43	387.35	450.89	463.46	521.72
		3.0	217.64	343.22	357.63	448.80	513.60	524.26	567.84	624.71	685.58	708.75
		5.0	268.10	424.65	436.55	552.02	625.25	631.85	700.08	750.21	843.55	848.44
		6.0	289.93	459.41	470.64	595.80	673.22	678.81	756.13	803.82	908.98	910.37
2.0	50	1.0	244.18	299.35	381.63	482.47	569.61	583.96	635.36	677.48	752.81	791.04
		3.0	314.12	393.79	506.41	637.50	679.16	731.02	795.19	831.19	949.89	964.64
		5.0	370.62	466.24	599.74	751.60	773.48	835.70	931.92	948.31	1098.20	1110.03
		6.0	395.40	497.67	639.94	799.21	817.36	881.59	991.81	999.74	1156.66	1180.21
	60	1.0	253.96	312.02	397.81	502.02	582.35	603.88	652.29	696.81	774.93	812.20
		3.0	332.81	417.65	537.04	675.12	708.96	765.01	839.20	869.04	1001.42	1007.78
		5.0	395.68	497.89	640.12	799.35	817.50	881.72	991.93	999.85	1156.76	1180.31
		6.0	423.12	532.58	684.39	850.10	868.40	932.86	1057.07	1058.17	1221.68	1258.08
	75	1.0	267.82	329.81	420.46	529.49	600.89	631.07	677.73	723.75	807.37	842.06
		3.0	358.66	450.45	579.00	726.25	751.47	811.92	900.55	921.53	1067.56	1073.15
		5.0	430.04	541.14	695.14	862.11	881.01	945.26	1070.89	1074.08	1237.30	1276.71
		6.0	461.01	580.19	744.88	917.46	940.88	1003.48	1135.89	1148.72	1310.88	1364.51
	90	1.0	280.86	346.38	441.52	555.09	618.79	655.53	703.13	748.76	838.81	870.06
		3.0	382.44	480.46	617.27	772.13	792.02	855.21	957.12	970.00	1122.69	1139.32
		5.0	461.38	580.48	745.11	917.64	941.06	1003.65	1136.04	1148.86	1311.01	1364.63
		6.0	495.48	623.44	799.77	978.08	1007.93	1068.22	1208.02	1230.94	1392.33	1461.30

Table 8: Natural frequency parameter of skew plate, B.C.- SSSS, $\beta = 45^{o}$, $v_s = 0.20$, $\rho_s = 1700$ kg/m³ and $\gamma = 1$

a/b	E_s (MN/m²)	H (m)	τ_1	τ_2	τ_3	τ_4	τ_5	τ_6	τ_7	τ_8	τ_9	τ_{10}
0.5	50	1.0	42.07	55.18	74.03	95.43	102.16	110.93	124.04	130.95	151.23	157.99
		3.0	61.17	80.17	106.38	130.59	137.71	145.88	170.05	170.37	202.45	204.31
		5.0	75.98	98.83	130.12	155.61	166.78	172.88	200.14	205.55	236.45	245.06
		6.0	82.36	106.85	140.27	166.55	179.31	184.72	213.28	220.70	251.26	262.69
	60	1.0	44.97	58.71	78.36	100.35	106.17	115.36	129.66	135.80	157.58	163.44
		3.0	66.14	86.37	114.21	138.73	147.19	154.64	179.80	181.85	213.47	217.54
		5.0	82.45	106.91	140.32	166.60	179.34	184.75	213.31	220.73	251.29	262.72
		6.0	89.46	115.71	151.47	178.76	193.12	197.89	227.88	237.38	267.68	282.17
	75	1.0	48.97	63.58	84.37	107.02	112.06	121.55	137.69	142.63	166.65	171.13
		3.0	72.93	94.83	124.89	149.98	160.24	166.77	193.29	197.59	228.69	235.76
		5.0	91.24	117.89	154.18	181.71	196.44	201.07	231.40	241.38	271.62	286.82
		6.0	99.10	127.75	166.67	195.51	211.87	215.95	247.89	260.04	290.13	308.67
	90	1.0	52.66	68.05	89.89	112.97	117.87	127.33	145.25	149.03	175.21	178.33
		3.0	79.10	102.51	134.58	160.34	172.15	177.95	205.71	211.96	242.68	252.45
		5.0	99.21	127.83	166.73	195.56	211.92	216.00	247.94	260.09	290.16	308.70
		6.0	107.81	138.63	180.41	210.81	228.83	232.44	266.14	280.54	310.57	332.68
1.0	50	1.0	105.89	158.43	178.02	209.22	259.19	266.44	282.63	327.28	328.47	382.34
		3.0	149.82	237.91	252.07	314.60	366.65	379.66	400.25	453.31	487.10	520.73
		5.0	187.30	298.26	310.11	391.48	448.27	456.95	497.74	546.28	603.06	621.35
		6.0	203.58	324.12	335.27	424.19	483.55	490.95	539.32	586.08	652.55	665.27
	60	1.0	114.80	170.71	189.14	224.30	273.73	284.58	295.43	343.94	349.20	402.08
		3.0	163.05	258.26	271.51	340.27	393.55	404.90	432.49	483.97	525.27	553.51
		5.0	204.13	324.47	335.61	424.45	483.79	491.18	539.53	586.28	652.72	665.44
		6.0	221.95	352.81	363.32	460.22	522.68	528.94	585.08	629.99	706.94	714.13
	75	1.0	126.96	187.51	204.58	244.96	294.00	309.58	313.49	367.13	378.00	427.98
		3.0	181.00	285.90	298.13	375.06	430.44	439.91	476.33	525.78	577.26	598.74
		5.0	226.92	359.99	370.36	469.04	532.23	538.26	596.14	640.62	720.01	725.97
		6.0	246.81	391.63	401.48	508.93	575.93	581.04	647.01	689.63	780.54	781.08
	90	1.0	138.01	202.85	218.85	263.82	312.79	330.43	332.50	388.59	404.56	450.96
		3.0	197.25	310.94	322.42	406.50	464.12	472.21	516.06	563.76	624.42	640.33
		5.0	247.50	392.06	401.91	509.27	576.23	581.33	647.27	689.88	780.76	781.30
		6.0	269.23	426.65	436.07	552.85	624.23	628.57	702.89	743.67	842.14	846.90
2.0	50	1.0	168.14	220.78	296.38	381.84	408.15	443.42	496.46	523.96	605.29	632.32
		3.0	244.55	320.70	425.83	521.65	551.21	582.98	680.13	681.98	810.20	817.68
		5.0	303.76	395.36	520.83	621.51	667.75	690.79	800.26	823.01	946.19	981.01
		6.0	329.28	427.41	561.48	665.18	717.98	738.00	852.72	883.76	1005.39	1051.75
	60	1.0	179.73	234.87	313.72	401.41	424.26	461.12	518.96	543.36	630.67	654.16
		3.0	264.44	345.51	457.18	554.16	589.25	617.93	719.06	727.96	854.27	870.67
		5.0	329.63	427.68	561.69	665.35	718.14	738.15	852.85	883.89	1005.50	1051.86
		6.0	357.66	462.88	606.33	713.85	773.38	790.55	911.03	950.76	1071.05	1129.91
	75	1.0	195.75	254.35	337.75	427.93	448.03	485.84	551.07	570.65	666.91	684.93
		3.0	291.59	379.34	499.90	599.05	641.56	666.37	772.93	791.08	915.16	943.72
		5.0	364.78	471.58	617.19	725.64	786.70	803.25	925.07	966.79	1086.80	1148.60
		6.0	396.16	511.02	667.19	780.60	848.63	862.58	990.88	1041.80	1160.83	1236.39
	90	1.0	210.49	272.25	359.86	451.58	471.45	508.89	581.36	596.19	701.17	713.76
		3.0	316.26	410.08	538.71	640.38	689.30	711.01	822.51	848.69	971.10	1010.64
		5.0	396.59	511.35	667.45	780.81	848.83	862.78	991.05	1041.96	1160.98	1236.52
		6.0	430.96	554.57	722.26	841.52	916.73	928.28	1063.69	1124.23	1242.60	1332.96

Table 9: Natural frequency parameter of skew plate, B.C.- FFFF, $\beta = 45^0$, $v_s = 0.20$, $\rho_s = 1700$ kg/m³ and $\gamma = 1$

a/b	E_s (MN/m²)	H (m)	τ_1	τ_2	τ_3	τ_4	τ_5	τ_6	τ_7	τ_8	τ_9	τ_{10}
0.5	50	1.0	24.68	32.83	44.94	46.99	54.62	58.75	68.20	73.48	83.57	89.06
		3.0	25.25	40.55	62.11	62.97	74.63	85.58	95.30	109.00	118.83	126.42
		5.0	26.93	47.40	75.46	75.91	89.86	105.37	115.00	134.45	144.84	152.94
		6.0	27.73	50.43	81.23	81.57	96.46	113.82	123.45	145.24	156.02	164.28
	60	1.0	26.91	35.69	48.77	51.02	59.04	63.67	73.35	79.38	89.69	95.74
		3.0	27.55	44.12	67.51	68.47	80.77	92.98	102.73	118.19	128.28	135.89
		5.0	29.35	51.58	82.08	82.62	97.41	114.56	124.22	145.91	156.77	164.88
		6.0	30.21	54.88	88.38	88.81	104.62	123.77	133.46	157.64	169.01	177.30
	75	1.0	29.93	39.55	53.93	56.42	64.96	70.31	80.24	87.38	97.96	104.24
		3.0	30.65	48.95	74.81	75.89	89.06	102.97	112.74	130.58	141.07	148.68
		5.0	32.62	57.22	91.02	91.68	107.61	126.96	136.68	161.33	172.89	181.04
		6.0	33.56	60.88	98.03	98.59	115.65	137.19	146.99	174.33	186.56	194.90
	90	1.0	32.66	43.04	58.56	61.25	70.25	76.30	86.41	94.60	105.42	111.61
		3.0	33.46	53.30	81.38	82.58	96.53	111.96	121.74	141.72	152.60	160.21
		5.0	35.56	62.30	99.07	99.86	116.81	138.11	147.92	175.17	187.44	195.62
		6.0	36.57	66.28	106.71	107.41	125.60	149.25	159.21	189.32	202.40	210.81
1.0	50	1.0	81.36	113.86	120.83	144.84	169.99	182.16	183.59	207.65	225.62	248.13
		3.0	79.43	140.59	146.84	192.72	231.57	246.27	263.17	286.57	333.78	349.89
		5.0	83.33	165.05	172.39	230.94	281.79	299.01	323.06	346.38	412.16	427.61
		6.0	85.34	175.89	183.93	247.57	303.77	322.11	348.75	372.25	445.42	461.27
	60	1.0	88.87	124.13	130.91	157.51	184.12	195.71	199.54	224.11	244.63	266.40
		3.0	86.79	153.46	159.78	209.64	251.90	266.46	286.47	309.94	362.68	378.12
		5.0	90.97	180.09	187.86	251.29	306.99	324.49	351.76	375.31	447.98	463.50
		6.0	93.11	191.87	200.50	269.42	331.06	349.84	379.75	403.62	484.17	500.42
	75	1.0	99.06	138.04	144.55	174.60	203.16	213.99	221.10	246.14	270.37	291.01
		3.0	96.75	170.84	177.34	232.48	279.42	293.92	317.90	341.46	401.62	416.41
		5.0	101.28	200.35	208.81	278.76	341.08	359.06	390.46	414.43	496.20	512.15
		6.0	103.60	213.38	222.95	298.91	367.96	387.44	421.55	446.08	536.35	553.46
	90	1.0	108.28	150.61	156.89	190.00	220.29	230.51	240.56	265.84	293.61	313.17
		3.0	105.74	186.51	193.24	253.08	304.29	318.82	346.22	369.86	436.63	451.08
		5.0	110.58	218.58	227.75	303.52	371.84	390.34	425.28	449.77	539.53	556.12
		6.0	113.06	232.73	243.22	325.47	401.24	421.41	459.14	484.42	583.23	601.37
2.0	50	1.0	98.70	131.37	179.81	187.93	218.54	235.05	273.01	293.96	334.26	356.31
		3.0	100.99	162.23	248.53	251.82	298.53	342.42	381.41	436.14	475.24	505.69
		5.0	107.70	189.62	301.92	303.54	359.45	421.61	460.24	538.02	579.25	611.77
		6.0	110.94	201.76	325.03	326.18	385.82	455.44	494.05	581.18	623.95	657.14
	60	1.0	107.62	142.80	195.14	204.05	236.22	254.74	293.60	317.58	358.71	383.04
		3.0	110.18	176.51	270.14	273.80	323.09	372.03	411.14	472.92	513.05	543.59
		5.0	117.39	206.35	328.43	330.35	389.61	458.42	497.13	583.87	626.91	659.56
		6.0	120.86	219.56	353.66	355.10	418.43	495.31	534.10	630.85	675.84	709.20
	75	1.0	119.70	158.25	215.78	225.63	259.88	281.32	321.18	349.58	391.80	416.90
		3.0	122.62	195.82	299.32	303.46	356.24	412.00	451.17	522.50	564.16	594.75
		5.0	130.47	228.93	364.22	366.57	430.39	508.06	546.97	645.61	691.36	724.17
		6.0	134.25	243.57	392.30	394.14	462.53	549.04	588.27	697.69	746.01	779.64
	90	1.0	130.63	172.18	234.34	244.94	281.04	305.27	345.83	378.47	421.63	446.41
		3.0	133.84	213.24	325.62	330.20	386.12	447.99	487.17	567.10	610.26	640.85
		5.0	142.26	249.28	396.47	399.21	467.18	552.73	591.97	701.06	749.52	782.50
		6.0	146.30	265.20	427.10	429.32	502.30	597.37	637.21	757.72	809.31	843.24

Table 10: Natural frequency parameter of skew plate, B.C.- CCCC, $\beta = 60^0$, $v_s = 0.20$, $\rho_s = 1700$ kg/m³ and $\gamma = 1$

a/b	E_s (MN/m²)	H (m)	τ_1	τ_2	τ_3	τ_4	τ_5	τ_6	τ_7	τ_8	τ_9	τ_{10}
0.5	50	1.0	50.17	62.20	80.34	102.94	108.40	117.28	130.79	133.90	157.23	160.08
		3.0	69.26	86.95	111.96	139.53	142.54	152.57	172.92	175.94	200.44	211.65
		5.0	84.23	105.84	135.79	165.60	171.37	180.46	203.76	210.52	234.69	251.68
		6.0	90.74	114.01	146.10	177.00	183.95	192.73	217.34	225.54	249.78	269.15
	60	1.0	52.94	65.59	84.49	107.78	112.36	121.60	136.31	138.60	162.37	166.25
		3.0	74.25	93.18	119.77	148.02	151.87	161.58	182.87	187.17	211.47	224.59
		5.0	90.81	114.07	146.15	177.04	183.99	192.77	217.37	225.57	249.81	269.17
		6.0	97.99	123.09	157.53	189.72	197.91	206.42	232.47	242.19	266.62	288.54
	75	1.0	56.82	70.32	90.27	114.53	118.07	127.74	144.13	145.32	169.73	175.04
		3.0	81.10	101.74	130.50	159.72	164.83	174.11	196.71	202.65	226.81	242.50
		5.0	99.80	125.32	160.30	192.79	201.27	209.73	236.12	246.18	270.68	293.18
		6.0	107.86	135.47	173.13	207.18	216.99	225.23	253.29	264.95	289.81	315.09
	90	1.0	60.42	74.71	95.64	120.74	123.57	133.54	151.48	151.67	176.70	183.34
		3.0	87.36	109.55	140.30	170.50	176.75	185.69	209.51	216.85	241.02	258.98
		5.0	107.96	135.55	173.19	207.24	217.04	225.28	253.33	264.99	289.84	315.12
		6.0	116.83	146.72	187.31	223.16	234.37	242.44	272.34	285.69	311.05	339.30
1.0	50	1.0	114.61	172.16	182.42	224.99	263.33	271.92	287.17	325.05	352.78	375.98
		3.0	160.16	253.26	259.66	329.50	374.38	377.69	420.81	449.13	510.36	512.00
		5.0	198.47	314.88	319.85	406.73	458.83	460.67	519.33	542.69	617.67	619.90
		6.0	215.13	341.37	345.92	439.88	495.37	496.86	561.62	583.27	663.85	665.80
	60	1.0	123.49	184.44	193.89	239.76	278.26	285.81	305.04	341.37	373.21	393.11
		3.0	173.59	273.95	279.79	355.15	402.17	404.87	453.27	479.78	546.35	548.48
		5.0	215.66	341.70	346.25	440.13	495.60	497.08	561.82	583.46	664.02	665.97
		6.0	233.93	370.80	374.97	476.57	535.91	537.12	608.32	628.34	715.21	716.98
	75	1.0	135.63	201.30	209.81	260.08	299.08	305.41	329.79	364.13	401.65	417.30
		3.0	191.84	302.13	307.35	390.10	440.31	442.39	497.57	521.90	593.86	596.30
		5.0	238.97	378.15	382.23	485.56	545.79	546.96	619.63	639.28	727.64	729.38
		6.0	259.42	410.74	414.50	526.45	591.14	592.15	671.82	689.96	785.55	787.22
	90	1.0	146.71	216.72	224.51	278.68	318.39	323.79	352.57	385.23	427.94	439.98
		3.0	208.40	327.71	332.47	421.85	475.16	476.83	537.88	560.46	637.58	639.68
		5.0	260.08	411.15	414.91	526.77	591.43	592.44	672.07	690.20	785.77	787.44
		6.0	282.48	446.89	450.36	571.65	641.30	642.25	729.37	746.09	849.68	851.40
2.0	50	1.0	200.50	248.74	321.53	412.01	432.90	468.59	523.60	535.35	629.12	640.80
		3.0	276.85	347.74	447.98	557.46	570.39	609.60	691.25	704.40	801.79	847.37
		5.0	336.71	423.26	543.32	661.42	685.91	720.96	814.44	842.92	938.61	1007.80
		6.0	362.68	455.94	584.56	706.88	736.30	769.92	868.62	903.13	998.90	1077.87
	60	1.0	211.59	262.32	338.10	431.34	448.79	485.86	545.68	554.15	649.68	665.50
		3.0	296.81	372.67	479.24	591.31	607.83	645.60	731.00	749.37	845.83	899.22
		5.0	363.00	456.19	584.76	707.04	736.46	770.07	868.75	903.25	999.02	1077.97
		6.0	391.63	492.24	630.30	757.55	792.23	824.51	929.03	969.89	1066.18	1155.68
	75	1.0	227.10	281.24	361.24	458.25	471.73	510.40	576.99	580.97	679.07	700.69
		3.0	324.19	406.88	522.14	637.97	659.74	695.63	786.27	811.39	907.16	971.01
		5.0	398.85	501.14	641.39	769.82	805.71	837.70	943.60	985.93	1082.39	1174.33
		6.0	431.04	541.71	692.70	827.10	868.68	899.48	1012.07	1061.22	1158.80	1262.30
	90	1.0	241.50	298.78	382.72	482.96	493.88	533.58	606.37	606.44	706.94	733.94
		3.0	349.20	438.12	561.36	680.96	707.46	741.85	837.36	868.32	963.92	1037.10
		5.0	431.44	542.03	692.95	827.31	868.88	899.67	1012.24	1061.38	1158.95	1262.43
		6.0	466.81	586.65	749.46	890.65	938.33	968.02	1088.04	1144.46	1243.67	1359.60

Table 11: Natural frequency parameter of skew plate, B.C.- SSSS, $\beta = 60^0$, $v_s = 0.20$, $\rho_s = 1700$ kg/m³ and $\gamma = 1$

a/b	E_s (MN/m²)	H (m)	τ_1	τ_2	τ_3	τ_4	τ_5	τ_6	τ_7	τ_8	τ_9	τ_{10}
0.5	50	1.0	38.69	50.04	66.79	82.33	87.97	92.27	108.61	111.71	131.55	137.40
		3.0	58.67	75.74	99.43	117.24	127.68	129.75	149.62	158.72	176.51	190.90
		5.0	74.00	94.99	123.66	144.05	157.27	158.58	181.31	193.98	211.46	231.21
		6.0	80.59	103.27	134.08	155.72	170.02	171.13	195.14	209.21	226.77	247.20
	60	1.0	41.76	53.69	71.18	86.79	93.08	96.98	113.68	117.59	137.01	143.93
		3.0	63.82	82.13	107.41	125.98	137.36	139.13	159.90	170.21	187.81	204.12
		5.0	80.68	103.34	134.14	155.76	170.06	171.17	195.18	209.25	226.80	247.23
		6.0	87.93	112.45	145.62	168.67	184.13	185.07	210.51	226.06	243.80	265.11
	75	1.0	45.98	58.73	77.25	93.06	100.22	103.63	120.84	125.85	144.76	153.15
		3.0	70.85	90.86	118.31	138.04	150.63	152.08	174.11	186.00	203.47	222.35
		5.0	89.77	114.70	148.41	171.81	187.53	188.43	214.21	230.10	247.90	269.44
		6.0	97.89	124.91	161.32	186.38	203.37	204.13	231.57	249.03	267.20	289.87
	90	1.0	49.83	63.34	82.84	98.92	106.83	109.86	127.57	133.55	152.06	161.81
		3.0	77.22	98.80	128.25	149.10	162.74	163.96	187.19	200.43	217.90	237.91
		5.0	97.99	125.00	161.38	186.44	203.42	204.18	231.61	249.07	267.24	289.91
		6.0	106.90	136.21	175.57	202.52	220.84	221.51	250.78	269.92	288.59	312.62
1.0	50	1.0	102.16	151.00	158.67	196.85	229.27	235.71	252.11	283.50	310.82	328.35
		3.0	146.98	232.18	237.36	301.89	342.60	345.11	386.51	410.45	468.52	469.45
		5.0	185.33	293.98	298.15	379.49	427.90	429.32	485.27	505.33	575.82	577.65
		6.0	202.00	320.52	324.38	412.75	464.68	465.82	527.61	546.32	622.47	624.07
	60	1.0	111.28	163.57	170.70	211.95	244.82	250.46	270.34	300.47	331.66	346.32
		3.0	160.50	253.00	257.78	327.72	370.77	372.82	419.10	441.62	503.52	505.95
		5.0	202.56	320.87	324.73	413.02	464.92	466.07	527.82	546.53	622.65	624.25
		6.0	220.84	349.99	353.57	449.55	505.42	506.35	574.35	591.78	674.26	675.68
	75	1.0	123.69	180.77	187.27	232.63	266.37	271.09	295.47	324.01	360.54	371.54
		3.0	178.86	281.30	285.64	362.87	409.30	410.90	463.54	484.34	551.76	553.76
		5.0	225.92	357.37	360.88	458.58	515.36	516.25	585.68	602.81	686.79	688.17
		6.0	246.35	389.96	393.23	499.52	560.87	561.61	637.87	653.80	745.05	746.33
	90	1.0	134.95	196.43	202.45	251.49	286.24	290.26	318.52	345.73	387.13	395.06
		3.0	195.47	306.97	310.98	394.77	444.43	445.72	503.92	523.36	596.00	597.73
		5.0	247.04	390.39	393.66	499.86	561.17	561.91	638.13	654.06	745.28	746.55
		6.0	269.41	426.11	429.15	544.78	611.18	611.81	695.41	710.21	809.50	810.72
2.0	50	1.0	154.69	200.17	267.38	328.73	352.22	368.64	434.37	447.29	526.64	550.12
		3.0	234.61	302.96	397.90	468.44	511.12	518.61	598.32	635.47	706.34	764.24
		5.0	295.94	379.99	494.81	575.70	629.50	633.91	725.04	776.65	846.08	923.18
		6.0	322.33	413.11	536.52	622.36	680.56	684.10	780.35	837.65	907.29	987.05
	60	1.0	166.98	214.79	284.92	346.59	372.67	387.51	454.62	470.85	548.47	576.24
		3.0	255.24	328.55	429.81	503.42	549.86	556.14	639.43	681.48	751.51	817.17
		5.0	322.68	413.39	536.73	622.54	680.72	684.27	780.49	837.78	907.41	987.17
		6.0	351.66	449.81	582.67	674.15	737.03	739.82	841.81	905.12	975.42	1058.59
	75	1.0	183.85	234.93	309.21	371.68	401.23	414.12	483.27	503.90	579.45	613.16
		3.0	283.34	363.46	473.42	551.65	602.95	607.91	696.26	744.67	814.12	889.96
		5.0	359.01	458.82	593.86	686.67	750.64	753.27	856.61	921.31	991.82	1075.85
		6.0	391.48	499.68	645.50	744.93	814.04	816.03	926.00	997.18	1068.98	1157.40
	90	1.0	199.28	253.40	331.56	395.12	427.70	439.03	510.19	534.70	608.63	647.79
		3.0	308.85	395.20	513.16	595.89	651.42	655.45	748.54	802.45	871.85	949.93
		5.0	391.91	500.02	645.76	745.16	814.25	816.24	926.18	997.35	1069.14	1157.54
		6.0	427.52	544.89	702.53	809.38	884.03	885.46	1002.81	1080.90	1154.54	1248.15

Table 12: Natural frequency parameter of skew plate, B.C.- FFFF, $\beta = 60^0$, $v_s = 0.20$, $\rho_s = 1700$ kg/m³ and $\gamma = 1$

a/b	E_s (MN/m²)	H (m)	τ_1	τ_2	τ_3	τ_4	τ_5	τ_6	τ_7	τ_8	τ_9	τ_{10}
0.5	50	1.0	23.20	30.74	42.55	43.75	50.06	56.68	61.89	71.42	77.12	81.07
		3.0	23.53	38.54	59.92	60.25	70.09	83.59	88.14	106.04	112.72	117.17
		5.0	25.15	45.57	73.61	73.62	85.71	103.68	108.03	131.19	139.23	144.02
		6.0	25.95	48.70	79.47	79.56	92.49	112.30	116.67	141.94	150.67	155.63
	60	1.0	25.35	33.49	46.19	47.53	54.19	61.37	66.61	77.03	82.97	86.77
		3.0	25.70	42.03	65.25	65.66	76.17	90.92	95.40	114.99	122.09	126.50
		5.0	27.43	49.70	80.26	80.33	93.29	112.93	117.28	142.52	151.23	156.08
		6.0	28.29	53.11	86.74	86.77	100.73	122.36	126.79	154.29	163.80	168.86
	75	1.0	28.27	37.21	51.11	52.64	59.77	67.74	72.97	84.64	90.89	94.50
		3.0	28.64	46.75	72.49	73.00	84.41	100.87	105.26	127.11	134.80	139.20
		5.0	30.52	55.28	89.26	89.42	103.57	125.45	129.85	157.87	167.53	172.49
		6.0	31.45	59.07	96.53	96.59	111.89	135.97	140.54	171.02	181.64	186.86
	90	1.0	30.90	40.58	55.57	57.25	64.81	73.50	78.71	91.53	98.03	101.49
		3.0	31.29	51.01	79.03	79.64	91.86	109.86	114.20	138.06	146.32	150.74
		5.0	33.30	60.31	97.39	97.64	112.87	136.75	141.27	171.74	182.30	187.40
		6.0	34.29	64.44	105.35	105.49	121.98	148.26	153.01	186.14	197.80	203.19
1.0	50	1.0	78.29	109.12	111.85	137.38	159.22	164.61	177.34	190.33	218.97	227.77
		3.0	74.77	136.31	139.07	184.72	223.52	233.37	257.27	268.04	324.55	333.21
		5.0	78.16	161.71	165.32	223.79	275.58	288.61	318.47	328.94	402.52	413.91
		6.0	80.04	173.02	177.12	240.89	298.31	312.63	344.88	355.47	435.99	448.81
	60	1.0	85.65	119.13	121.74	149.50	172.85	178.01	192.72	205.54	237.15	245.34
		3.0	81.76	148.95	151.81	201.38	243.79	253.93	280.41	291.02	352.81	361.74
		5.0	85.37	176.66	180.61	244.12	300.96	314.61	347.42	357.99	438.19	450.53
		6.0	87.38	188.99	193.53	262.82	325.90	340.95	376.32	387.13	474.85	488.87
	75	1.0	95.63	132.71	135.18	165.91	191.34	196.25	213.58	226.10	261.81	269.22
		3.0	91.21	166.05	169.10	223.95	271.29	281.88	311.76	322.25	391.08	400.55
		5.0	95.10	196.86	201.32	271.64	335.37	349.88	386.60	397.44	486.51	500.27
		6.0	97.28	210.56	215.76	292.49	363.29	379.35	418.86	430.12	527.50	543.25
	90	1.0	104.65	145.01	147.37	180.75	208.08	212.82	232.46	244.68	284.13	290.88
		3.0	99.75	181.48	184.75	244.35	296.19	307.21	340.10	350.57	425.67	435.77
		5.0	103.88	215.07	220.05	296.49	366.50	381.79	421.99	433.19	530.20	545.32
		6.0	106.21	230.00	235.86	319.28	397.10	414.07	457.26	469.06	575.09	592.48
2.0	50	1.0	92.81	122.99	170.25	174.93	200.22	226.74	247.74	285.71	308.37	324.40
		3.0	94.14	154.16	239.71	240.94	280.36	334.39	352.70	424.20	450.82	468.73
		5.0	100.59	182.31	294.43	294.48	342.82	414.76	432.25	524.80	556.86	576.10
		6.0	103.79	194.80	317.82	318.27	369.96	449.24	466.81	567.81	602.63	622.53
	60	1.0	101.40	133.97	184.80	190.08	216.75	245.53	266.58	308.13	331.80	347.18
		3.0	102.82	168.12	261.05	262.60	304.65	363.73	381.71	459.98	488.29	506.04
		5.0	109.73	198.82	321.07	321.26	373.15	451.75	469.24	570.12	604.86	624.32
		6.0	113.16	212.44	346.90	347.12	402.90	489.47	507.28	617.21	655.16	675.43
	75	1.0	113.06	148.86	204.50	210.51	239.07	271.00	292.01	338.57	363.47	378.09
		3.0	114.56	187.00	289.98	291.96	337.61	403.50	421.14	508.46	539.15	556.82
		5.0	122.07	221.14	357.09	357.61	414.28	501.82	519.56	631.51	670.06	689.95
		6.0	125.80	236.28	386.19	386.27	447.54	543.92	562.31	684.13	726.51	747.40
	90	1.0	123.60	162.34	222.32	228.94	259.23	294.04	314.96	366.16	392.04	406.05
		3.0	125.15	204.06	316.14	318.51	367.43	439.46	456.91	552.28	585.24	602.96
		5.0	133.19	241.27	389.64	390.46	451.47	547.05	565.22	687.00	729.16	749.54
		6.0	137.19	257.78	421.49	421.84	487.90	593.07	612.24	744.63	791.17	812.71